

1 Quantifying the effect of solution formulation on the removal of soft solid food  
2 deposits from stainless steel substrates

3 Cuckston, G.L.<sup>1</sup>, Alam, Z.<sup>2</sup>, Goodwin, J.<sup>2</sup>, Ward, G.<sup>2</sup> and Wilson, D.I.<sup>1</sup>

4 <sup>1</sup>Department of Chemical Engineering and Biotechnology, Philippa Fawcett Drive,  
5 Cambridge, CB3 0AS, UK

6 <sup>2</sup>Proctor & Gamble Technical Centres Ltd., Whitley Road, Longbenton, Newcastle-  
7 upon-Tyne NE12 9TS, UK

8  
9  
10 Submitted to

11  
12 *Journal of Food Engineering*

13  
14 Revised Manuscript

15 August 2018

16  
17 ©GLC, ZA, JG, GW and DIW

18  
19  
20  
21  
22 Corresponding author

23 D. Ian Wilson

24 Tel. +44 1223 334 791

25 E-mail: diw11@cam.ac.uk

# Quantifying the effect of solution formulation on the removal of soft solid food deposits from stainless steel substrates

Cuckston, G.L.<sup>1</sup>, Alam, Z.<sup>2</sup>, Goodwin, J.<sup>2</sup>, Ward, G.<sup>2</sup> and Wilson, D.I.<sup>1</sup>

<sup>1</sup>Department of Chemical Engineering and Biotechnology, Philippa Fawcett Drive, Cambridge, CB3 0AS, UK

<sup>2</sup>Proctor & Gamble Technical Centres Ltd., Whitley Road, Longbenton, Newcastle-upon-Tyne NE12 9TS, UK

## *Abstract*

The role of detergent formulation on the cleaning of a complex carbohydrate-fat food soil from stainless steel surfaces was studied using a modified version of the millimanipulation device described by Ali *et al.* (2015b) which allowed the force required to scrape the soil from the surface to be measured as the soil is immersed, in situ and in real time. This allowed the influence of temperature, solution chemistry and time on the mechanical forces (rheology) and removal behaviour of the soil to be studied – in effect quantifying the relationships in Sinner’s cleaning circle. The soil simulated a burnt-on baked-on deposit and featured regular cracking in the 300 µm thick layer. The removal force decreased noticeably on hydration: the cleaning mechanism was then determined by the agents present. At 20°C, below the temperature at which the fat phase was mobile, removal was characterised by cohesive failure except in the presence of the cationic surfactant CTAB, which promoted adhesive failure and fast decay in removal force. At 50°C, when the fat was mobile, a transition between cohesive and adhesive failure was observed at pH 7 which was inhibited at higher pH. Adhesive failure and fast decay in removal force was observed at higher pH and 50°C in the presence of the anionic and non-ionic surfactants, SDBS and TX-100, respectively.

**Keywords** Millimanipulation, cleaning, adhesion, burnt soil, surfactant

## **Introduction**

Fouling and cleaning is ubiquitous in the food sector, from the domestic kitchen to large scale manufacturing plants. The first commercially available electrical dishwasher was

56 sold in the 1920s and improvements to their effectiveness have been achieved both by  
57 optimising the water cycling system (e.g. Rosa *et al*, 2012) and developing  
58 combinations of cleaning agents in the ‘detergent’ to clean more quickly and impart  
59 dishes with ‘shine’ (Showell, 2005; Rosen and Kunjappu, 2012).

60 Significant advances have been made in the understanding of the cleaning mechanisms  
61 of single-component food soils over the past 20 years. Soils studied include whey  
62 protein gels (Saikhwan *et al*, 2010), heated egg white (Li *et al*, 2015), milk deposits  
63 generated during thermal processing (both pasteurisation and higher temperature  
64 operation, e.g. Morison and Thorpe, 2001), mixtures of commercially available cooking  
65 oils (Jurado-Alameda *et al*, 2015), and starches (Otto *et al*, 2016). The cleaning  
66 mechanism is dictated by the composition and structure of the soil (Fryer and  
67 Asteriadou, 2009) and those listed all differed noticeably.

68 For example, the wheat starches studied by Din and Bird (1996) were cleaned via  
69 enzymatic breakdown of the starch polymers into dextrins, oligosaccharides and sugars,  
70 each of which are more soluble in water than the parent molecule (Pongsawasdo and  
71 Murakami, 2010). Jurado-Alameda *et al*. (2015) found that surfactants such as linear  
72 alkylybenzylsulphonate (LAS) had little impact on the rate and extent of cleaning of  
73 dried potato starch residues on stainless steel fibres. In the absence of amylases, high  
74 pH and long soaking times were required for cleaning regardless of surfactant  
75 concentration. The use of heated solutions gave more benefit than other factors at room  
76 temperature. Such information is often discussed in terms of Sinner’s cleaning circle  
77 relating how time, temperature, chemistry and mechanical forces together determine  
78 how well and how fast different soils can be removed from a surface.

79 Protein-containing soils generated by cooking often contain thermally denatured gels.  
80 These swell and may be broken down following contact with alkali, and cleaning can  
81 involve dissolution or erosion, both of which can be diffusion limited (Morison 2002).  
82 The erosion of heated whey protein deposits can be enhanced by flow pulsing (Gillham  
83 *et al*, 2000) or regular switching between cleaning solutions (Christian and Fryer 2006).

84 Oils have been found to be the most difficult of all common foodstuffs to clean (Detry  
85 *et al*, 2007, 2009; Palmisano *et al*, 2011) owing to their inherent hydrophobicity and  
86 tendency to wet many dishwares preferentially to water. Fatty soils pose a particular  
87 challenge as most consumer detergents employ aqueous solutions. The active agent

must therefore be soluble (or encapsulated) in water, preferentially adsorb on to the soil surface, remove the soil from the substrate, and stabilise removed residues in the solution. Highly polymerised lipids such as those found in burnt oil soils have limited solubility in organic solutions and no recorded solubility in water (Ali *et al.*, 2015a). High pH or long soaking times are often required, in combination with mechanical shear, to remove such soils from the substrate (Dunstan and Fletcher, 2014). Surfactants can promote detachment of mobile components at the soil-substrate interface (Ali *et al.*, 2015a, 2015b). A combination of saponification, mechanical cleaning and surfactant action will be required to clean burnt oil soils as the existing literature does not report a single mechanism being entirely effective.

Other techniques promoting cleaning include modification of the substrate, either temporarily, such as adjusting the electrostatic charge of a stainless steel surface (Mauermann *et al.*, 2009) or permanently via coating (Ashokkumar and Adler-Nissen, 2011; Magens *et al.*, 2017). These approaches are suited for repeated processes where the soil and substrate operations do not change: with multi-product plant (or facilities such as a kitchen) one substrate may enhance cleaning of one soil and promote adhesion of another (Ali, 2015).

#### *Baking and drying*

The properties of the soil to be cleaned are determined both by its composition and its processing history, and particularly its thermal history (Fryer and Asteriadou, 2009). Thermal transformation is widely used in food processing (baking, drying, frying, ...) and exposure to high temperatures, often in humid environments, promotes evaporation, shrinkage, and chemical reactions including free radical polymerisation, condensation polymerisation and thermal decomposition. These structural changes encourage closer packing which increases the cohesive forces in the soil (Stanga, 2010). This paper considers baked mixtures of proteins, fats and starches (with small amounts of minerals and fibres).

Drying (typically at 85-90 °C for 1 hour) has been shown to increase soil adhesion. Marked increases in both the cohesive and adhesive strength of starch soils following water loss were reported in ultrasound cleaning studies by Stanga (2010) and dynamic mechanical analysis measurements by Jonhed *et al.* (2008). Surface energy studies by

Otto *et al.* (2016) demonstrated that whilst starch underwent structural changes during heating, whey and soy proteins exhibited a significantly larger response to heating as measured by UV-Vis photometry in a continuous flow cleaning system. Protein denaturation caused by heating for an hour at temperatures above 55 °C caused internal hydrophobic structures to become exposed, accompanied by a large shift in the Lifshitz-van der Waals component of the soils surface energy measured for those soils. This leads to strong wetting and adhesion on stainless steel surfaces. The additional exposure of internal binding groups such as sulfhydryl allows disulphide bridges to form on drying, forming denser, more cohesive soils on the substrate (Castner and Ratner, 2002).

In this work the soiling layers were baked at 204 °C for 7 minutes, so that virtually all the water initially present is evaporated off and the above structural changes are accompanied by reaction steps. These burnt complex soil layers pose particular challenges for cleaning and the aim of this work is to generate insights into how particular cleaning agents or mixtures thereof achieve soil weakening or removal of multi-phase soils comprising of burnt starch-protein-fats solid networks surrounded by more mobile fats.

### *Soil Adhesion Forces*

Sinner's circle allows information about cleaning to be linked qualitatively, and there is a need to quantify the effect of chemistry and temperature on removal. For soils which do not dissolve, the response to mechanical forces, *i.e.* their rheology, needs to be quantified, preferably *in situ* and in real time.

Cleaning ultimately involves disruption of soil-substrate bonds. Soils bind through a combination of Lifshitz-van der Waals, ionic and electrostatic forces (Moeller and Nirschl, 2017). In dry conditions Lifshitz-van der Waals tend to dominate (Kumar *et al.*, 2013) but when immersed in aqueous solution, electrostatic forces, influenced by factors such as pH and electrolyte concentration, play a larger role (Israelachvili, 1998). Prochaska *et al.* (2007) reported that cationic starches had a stronger binding potential to stainless steel than natural starch, and attributed this to differences in ionic interactions with the steel surface which, when submerged in water, acquire a negative

charge. Determining the impact of cleaning agents on the balance of all the above interactions provides insight into the cleaning mechanisms and thus development of more effective dishwashing formulations through targeted selection of agents for components which are difficult to remove (Basso *et al.*, 2017).

Measurement of the forces required to clean, *i.e.* detach elements of soil from a substrate in a given environment is currently performed at three length scales of investigation: the nano-, micro- and macro-scales.

Macroscale testing of cleaning performance is the most widespread approach as it underpins empirical investigation and supports direct transfer of results to practice. Cleaning-in-place (CIP) systems are widely used to ensure the hygiene of food manufacturing plant, and scaled down systems have been used to investigate such operations. Interpretation of the results in terms of cleaning mechanisms can require detailed analysis which is not always straightforward. The bath-substrate-flow system employed by Jurado-Alameda *et al.* (2015) allows the effect of solution formulation to be studied but the flow regime in the cell is complex so identifying the dependency on local flow velocity (and hydraulic forces) is difficult. Flow cells (*e.g.* Bishop, 1997; Detry *et al.*, 2007; 2009) are often used to study the impact of shear forces in cleaning as the fluid flow patterns are known or can be predicted numerically, so that the results can be related to the process scale.

At the other end of the spectrum, nano-scale investigations typically involve measuring the adhesive forces between well-defined elements of a test soil and a surface. Aktar *et al.* (2010) used an AFM cantilever to measure the adhesion force<sup>1</sup> associated with removal of caramel particles from stainless steel and recorded values in the range of 0.1-0.3 N m<sup>-1</sup>. Bobe *et al.* (2007) reported similar values, of 0.21 – 1.3 N m<sup>-1</sup>, for removal of yeast particles from stainless steel surfaces. These forces depended on particle size and the distance of the tip from the soil. Such techniques can provide valuable insight into the chemical and electrostatic forces active in soil-substrate binding, and in attachment of spores and bacteria (*e.g.* Lelièvre *et al.*, 2002).

---

<sup>1</sup> Adhesion forces are reported in N m<sup>-1</sup>: this quantity is equivalent to surface energy, in J m<sup>-2</sup>

Food soils tend to be multicomponent and microstructured, subject to variations in topology, morphology and electrostatic environments across the substrate at the length scale of 10 – 100  $\mu\text{m}$ . Additional information on interactions is required for such systems and researchers have therefore tended to focus at the micro-scale. Moeller and Nirschl (2017) deposited approximately 1000 particles of starch-based soil onto a stainless steel surface and measured the centrifugal force required to remove them. This allowed statistical treatment of the results from a test of reasonable duration. They found that the repeatability of the method was highly dependent upon the soil type and structure: the more complex the soil the lower the repeatability. In this paper tests are performed in triplicate in order to create higher confidence in the repeatability of the results. This number of tests does not support a rigorous statistical analysis.

Surface roughness has also been shown to lead to variability in testing at this length scale. Hauser (2008) reported a decrease in adhesive strength between soil and substrate with increasing roughness but also a decrease in cleaning efficiency in immersed systems. Bobe *et al.* (2007) pointed out that measures of roughness such as  $R_q$  provide no information about the ‘structure’ of the roughness elements, *e.g.* spherical vs cylindrical vs conical, which play an important role in adhesion. Quantifying roughness and relating it to adhesion forces continues to be an active topic of investigation, promoted by the advent of nano-fabrication and tailoring of surfaces (LaMarche, 2017).

A number of micro-scale devices have been developed for studying the forces involved in cleaning under chemical environments and differences between soil components. These typically involve imposing a known shear force or shear stress on the layer and measuring the resulting deformation, or imposing a deformation *etc.* Fluid dynamic gauging (FDG) is an example of the former and has been used to monitor the strength (Chew *et al.*, 2004) and swelling characteristics (Gordon *et al.*, 2010) of food soils when contacted with a variety of cleaning solutions. Whereas denatured whey proteins were reported to swell and erode in alkali, gelatin and egg proteins both swelled but both require shear forces to effect removal (Gordon *et al.*, 2010; Perez-Mohedano *et al.*, 2016). Ali *et al.* (2015a) observed little swelling with burnt oil soils in aqueous cleaning solutions and removal of these was characterised by a ‘cohesive blistering’ mechanism. The size and quantity of blisters formed per sample depended upon the solution pH and the shear forces generated by agitation of the solution.

The use of controlled deformation (effectively controlled strain) devices was pioneered by workers at Birmingham (Liu *et al.*, 2002) who adapted a micromanipulation device originally developed for studying individual yeast cells (Marmoushy *et al.*, 1998) to study the removal of biofilms and soil layers. Liu *et al.* (2002) identified and quantified different failure modes between soil types: baked tomato paste removal was dominated by its cohesive strength, exhibited by its detachment in chunks even after soaking in an external bath, while pure whey protein deposits exhibited predominately cohesive failure.<sup>2</sup>

Micromanipulation tends to work at scale of tens of microns, and the heterogeneity of food deposits prompted workers such as Ashokkumar and Adler-Nissen (2011) and Ali *et al.* (2015b) to develop ‘millimanipulation’ devices which could be used to study composite deposits, as well as hard layers which techniques such as FDG could not deform. Those workers considered dry deposit layers. In this work, the device presented by Magens *et al.* (2017) was adapted to allow immersion of the sample in cleaning solutions for controlled lengths of time, at temperatures ranging from 20 °C to 50 °C, mimicking the chemical environment in a domestic automatic dishwasher. The soil studied is a complex mixture of starch, protein and fat, representative of some encountered in practice. The measurements provide indications of the rheology and cleaning behaviour of the soil, immersed in cleaning solution, *in situ* and in real time and thereby provide direct quantification of the effects of the parameters in Sinner’s cleaning circle.

## Materials and Methods

### *Soils and substrates*

A model burnt soil deposit, henceforth referred to a complex model soil (CMS), was generated containing fats, carbohydrates and proteins as detailed in Table 1. This formulation was provided by Procter and Gamble to mimic consumer products known to pose difficulty in automatic dishwashers. The soil was applied as a slurry to stainless steel substrates, dried and baked.

---

<sup>2</sup> There is a difference in terminology between Liu *et al.* (2002) and this paper. Liu *et al.* described a soil as failing cohesively when the adhesive strength of the soil to the substrate is lower than the internal cohesive strength of the soil. Here, cohesive failure is used to describe the case when the cohesive strength of the soil is lower than the adhesive strength of the soil to the substrate.



Slurry preparation involved boiling the pasta in deionised water for 7 minutes before draining the liquid off and adding the solids to the fat emulsion (pre-heated to 50 °C), milk, cheese powder and salt. The mixture was then blended for 1.5 minutes at maximum speed on a household food processor (Cookworks, HA-3213) until it appeared homogenous to the eye. An excess of the slurry was placed on the sample plate and a wiping blade device (Supplementary Figure S1) similar to that reported by Glover *et al.* (2016) was used to generate a smooth layer of initial thickness  $\delta$ . The gap between the blade and the substrate is set by a pair of micrometers with a precision of  $\pm 1 \mu\text{m}$ : the dried layer was rougher than this owing to the inherent heterogeneity of the slurry.  $\delta$  was typically 300  $\mu\text{m}$  and the layer mass approximately 1.8 g, giving an initial coverage on 50×50 mm test plates of 0.72 kg m<sup>-2</sup>.

The sample was then left to dry in air (20°C, 48 % humidity) for 24 hours before being baked in air in a conventional oven at 204 °C for 7 minutes. Baked samples were left standing in ambient air to cool to room temperature before testing.

Differential scanning calorimetry (DSC, Supplementary Figure S2) indicated that the majority of volatiles in the CMS are lost in the drying stage of sample preparation. A broad melting peak was evident in the dried and burnt samples between 20 and 40°C, with a sharp exothermic peak at 20°C on cooling, which is attributed to the fat phase.

The effect of temperature on the fat component was evaluated by studying the rheology of the emulsion employed in the formulation over the range 10-60°C, spanning the temperatures employed in the cleaning tests. The fat present in the soil contains less water and its rheological behaviour will be affected by changes introduced by baking and components absorbed from other ingredients in the CMS, so these results are interpreted as indicators of the fat behaviour. Samples were tested in a Malvern Kinexus rheometer using a 40 mm diameter smooth 4° cone and plate configuration. Shear rate sweeps at 22°C indicated viscoplastic behaviour (see Supplementary Figure S3 inset) with a critical stress of approximately 160 Pa and a critical shear rate of around 1 s<sup>-1</sup>. Measurement of apparent viscosity were therefore made at 0.1 s<sup>-1</sup> at intervals of 5 K. The apparent viscosity decreased strongly with temperature until 40°C, above which it was almost insensitive to temperature and the behaviour was Newtonian. This was

interpreted as the temperature at which the fat phase in the soil was expected to become mobile (i.e. more free flowing). These observations are consistent with the DSC results.

The substrates were fabricated from 316 stainless steel. The data presented here were obtained using 50 mm square plates with thickness 3 mm and surface root mean square roughness,  $R_q = 1.6 \mu\text{m}$  (measured using a scanning confocal thickness sensor, Micro-Epsilon model IFS2405-3). Prior to applying the soil the substrates were cleaned by sonication for 10 minute periods in aqueous 1M NaOH, dishwashing solution (Fairy Liquid<sup>TM</sup> in reverse osmosis water,  $< 5 \text{ g L}^{-1}$ ) then acetone, scrubbing with a soft cloth following each sonication step. Cleaning was repeated if any residual soil was visible. After each test any remaining soil was removed using a plastic spatula and the plate left to soak in 1M NaOH/soap solution overnight and rinsed with deionised water before undergoing the procedure outlined above.

Figure 1 shows photographs of the soil layer before and after baking. Drying was accompanied by a loss of around 50 % of the initial soil mass, which is comparable with the water content of the mixture (Table 1). A further 10 wt.% was lost during baking and was accompanied by visible cracking of the layer (see Figure 1(b)). It was not possible to generate layers of this soil free from cracks but prolonging the drying time, such as allowing the moisture to evaporate overnight before baking, reduced the severity and size of the cracking. Thinner soiling layers ( $\delta_{\text{initial}} < 200 \mu\text{m}$ ) exhibited finer scale cracking patterns, as defined both by cracking frequency and width, than thicker ones ( $\delta_{\text{initial}} > 500 \mu\text{m}$ ), which is consistent with the literature on film cracking (Lee and Routh, 2004).

The crack pattern structure was quantified using two methods. The first was based on the fraction of the plate area occupied by cracks. This was calculated by converting a photograph into a binary image in Matlab<sup>TM</sup> (Figure 1(c)) and dividing the soiled region into ten equal strips. The fraction of cracked area was calculated for each strip, giving an average of 38.8% with a standard deviation of 5.3%. The second was to count the number of cracks along 9 equally-spaced gridlines (Figure 1(d)). This gave averages ( $\pm$  standard deviation) in the vertical and horizontal directions of  $19.0 \pm 3.0$  and  $21.2 \pm 2.6$ , respectively, corresponding to a crack spacing of approximately 2.5 mm.

### 305    *Millimanipulation flow system*

306    The millimanipulation device described by Magens *et al.* (2017) (Figure 2) was  
307    modified to include a solution circulation system. The sample is located on a computer-  
308    controlled translation stage (labelled E on the figure, Standa 103880) which moves the  
309    sample so that the layer is forced against the blade (B, 24.6 mm long) at set velocity  $V$ .  
310    The blade is mounted on the end of a frictionless pivot and the force imposed on the  
311    blade is measured by a force transducer (C). Upwards motion of the blade, which would  
312    affect the measurement, is inhibited by a counterweight (D). Further details of the  
313    device and its operation are given in Magens *et al.* (2017).

314    The sample mount is located within a stainless steel chamber (internal dimensions  
315    113×61×13 mm). The volume of solution volume held in the chamber after locating the  
316    sample is approximately 87 ml.

317    A stirred 1 litre jacketed vessel served as the solution reservoir. Liquid is delivered at a  
318    set flow rate by a peristaltic pump to the base of the sample chamber (marked I). The  
319    solution passes across the chamber and leaves via the outlet located on the far wall  
320    before draining back to the reservoir under gravity. The reservoir contents are heated  
321    by recirculation of hot water through the jacket. The temperature of the solution is  
322    monitored by a thermocouple located in the sample chamber. Changes to solution  
323    composition are made in the reservoir.

324    The tests reported here featured a solution flow rate of  $100 \text{ ml min}^{-1}$ , giving a space  
325    time of approximately 53 s. The time taken for a change in solution chemistry to take  
326    effect in the chamber was determined by a simple residence time test whereby the  
327    conductivity of the solution in the reservoir was altered by adding a 10 mL dose of 1 M  
328    NaOH and monitoring the conductivity of the liquid leaving the chamber. Figure 3  
329    shows that breakthrough is observed after approximately 30 seconds followed by a two-  
330    step change in conductivity which could be modelled approximately as plug flow (along  
331    the connecting tubing) in parallel with a mixing element. The inset in Figure 3 shows  
332    that the change in conductivity was complete after 150 s at this flow rate.

333

### 334    *Test protocol*

Cleaning solution was initially circulated through the empty chamber to bring it to the required temperature. The solution was allowed to drain and the sample swiftly mounted in place, dry, and the millimanipulation blade located to pass over the substrate with a 50  $\mu\text{m}$  gap. Solution was then reintroduced and pumped through the chamber at a rate of 100  $\text{ml min}^{-1}$ . Once the surface of the layer was immersed, the blade motion was initiated. The blade moved across the sample at velocity  $V$  for a set time  $t_s$  to give a total displacement  $X = Vt_s$ . The velocity and distance travelled can be set as required (see Magens *et al.*, 2017). In these tests  $V$  was 0.1  $\text{mm s}^{-1}$  and the force on the blade was recorded at 151 Hz. For ease of plotting, the data are truncated on a 1:100 basis. The removal force per unit width,  $F_w$ , was calculated from

$$F_w = \frac{\text{measured force}}{\text{blade width}} \quad [1]$$

Tests were performed in triplicate. Removal profiles such as Figure 6 feature the average value of  $F_w$  plotted against blade-soil displacement,  $x$ . Later profiles show  $F_w$  plotted against time in contact with cleaning solution: since  $V$  is constant in these tests, the abscissa is readily converted between  $x$  and  $t$ .

Interpretation of  $F_w$  measurements in terms of material parameters and relating these to cleaning applications requires some care, as outlined by Ali *et al.* (2015b). When removal occurs purely by adhesive failure,  $F_w$  provides a measure of the work required to peel a deposit away from a surface and this can be related to forces (or momentum) applied to a layer by a tool or a flow. When removal occurs by cohesive breakdown, a quantitative model of the deformation is needed to isolate the contributions from rheological parameters such as yield strength and elastic compression to the measured force. These material parameters then need to be compared with the forces imposed in the cleaning operation. For cleaning in pipe flows, these are typically related to fluid shear but in cleaning by impinging jets or liquid films, shear and extensional forces can act depending on the geometry and whether the liquid film is confined or has a free surface. At a coarse level,  $F_w$  can be used to gauge the change in material strength.

### *Test solutions*

Test solutions were prepared in batches using 1 L deionised water and the pH adjusted to 7, 9 or 12 using 1 M aqueous NaOH. Surfactant solutions were prepared at 1 wt. %

loading using sodium dodecyl benzene sulfonate (SDBS, anionic, critical micelle concentration (CMC)  $0.1 \text{ g L}^{-1}$  (Sanz *et al.* 2003), hexadecyltrimethylammonium bromide (CTAB, cationic, CMC  $0.334 \text{ g L}^{-1}$  (Previdello *et al.* 2006), and *t*-octylphenoxypolyethoxyethanol (TX-100, non-ionic; CMC  $0.0131 \text{ g L}^{-1}$  (Ruiz *et al.* 2001). The mixtures were prepared by stirring at  $50 \text{ }^{\circ}\text{C}$  for 30 minutes before being left to cool to room temperature.

## Results and Discussion

### *Effect of contact with cleaning solution for set time*

The impact of immersion was initially assessed by comparing  $F_w$  before and after the sample was contacted with cleaning solution for a set time. Dry samples prepared on discs or square plates were mounted in the solution chamber with no liquid present and  $F_w$  measured at  $V = 0.1 \text{ mm s}^{-1}$  for 200 s, giving  $X_{\text{dry}} = 20 \text{ mm}$  (region A in Figure 4). Solution was then introduced to the chamber for periods ranging from 1 - 60 min with the sample stationary, after which  $F_w$  was measured for a further 200 s, giving  $20 \text{ mm} < X_{\text{wet}} \leq 40 \text{ mm}$ . A section of undisturbed material 10 mm long remained. Figure 4(b) shows an example of a square plate following testing with 1 wt% SDBS solution at pH 10 and room temperature. There is a noticeable amount of residual material on the substrate in region A (dry removal) compared with region B (following soaking), indicating that the adhesion of the soil to the substrate had decreased significantly.

The change in soil behaviour was also evident in the behaviour of the removed oil. Figure 5(a) shows that, prior to soaking, removal is characterised by the ‘chipping’ away of small chunks of material by the blade. After soaking, the removed soil forms a weakly cohesively-bound heap ahead of blade (Figure 5(b)). The absence of much residual material on the substrate indicates that adhesion of the soil layer was reduced more than cohesive interactions within the layer.

The importance of mechanical action is demonstrated by the presence of the residual material in region A and the original soil layer in region C. These remained in place, unchanged, after soaking, indicating that the weak shear force associated with the solution flow was not large enough to disrupt either material.

The corresponding  $F_w$  profiles are shown in Figure 6. The dry profiles exhibit a cut-off at 430 N m<sup>-1</sup>, which is due to the maximum force that could be measured for this setting of the transducer. The range can be extended by adjusting the transducer position, at the expense of reducing the sensitivity for weaker layers. The oscillations evident in the dry  $F_w$  profiles arise from the cracked nature of the soils. Regions free of deposit do not contribute to the force on the blade, and the periodicity is roughly consistent with the average measured crack spacing of 2.3 mm (Figure 1(d)). The average value of  $F_w$  for dry samples was consistent between tests, at approximately 400 N m<sup>-1</sup> (1 s.f.). This is comparable with the  $F_w$  values reported by Ali *et al.* (2015b) for baked lard (up to 430 N m<sup>-1</sup> for oils cooked for 5 hr at 220°C).

The  $F_w$  profiles for samples soaked at pH 10 at room temperature in Figure 6(b) show similar oscillation, associated with inhomogeneous coverage, and a general reduction in absolute amplitude with time. The relative amplitude of oscillation is consistent at approximately 20 % of the mean  $F_w$  value indicating the impact of the cracking is consistent over the test duration. The values are larger than those reported by Akhtar *et al.* (2010) and Bobe *et al.* (2007) of 0.1 - 0.3 and 1.3 N m<sup>-1</sup> for fresh caramel and yeast layers, respectively. With extended soaking they approach those reported by Ali *et al.* (2015b) for unbaked oil soils with thickness ranging from 0.3 to 0.6 mm, of 0-20 N m<sup>-1</sup>.

The average  $F_w$  value is plotted against soaking time in Figure 7, normalised by the dry value. After 10 minutes of soaking there was virtually no variation in  $F_w$ . Much of the weakening of the adhesive forces occurred within the first 10 minutes of soaking, and there is a noticeable reduction in  $F_w$  for the test started after 5 minutes of soaking, indicating that changes were occurring over this timescale. Subsequent testing focused on shorter soaking periods, measuring  $F_w$  continuously for 500 s after the soil contacted the solution.

Figure 7 also shows the average  $F_w$  values measured after soaking in 1 wt% SDBS solution at the same temperature and pH. There is no significant effect of this anionic surfactant, as both data sets exhibit an almost exponential decay to  $F_{w,wet}/F_{w,dry} = 0.05$  after 10 minutes. The  $F_w$  value obtained with SDBS after 60 minutes was larger than at 10 minutes, which was attributed to this sample having swollen more and having

absorbed more water. Similar results were obtained for SDBS solutions at pH 11 and 12 (data not reported).

#### *Effect of contact with solution, continuous measurement: effect of temperature*

Figure 8(a) shows examples of removal profiles obtained with no pre-soaking in water at pH 7 and 20 °C, with no surfactant present. The initial  $F_w$  values are noticeably smaller than the average of 400 N m<sup>-1</sup> for dry deposits evident in Figure 6(a). This arises from the nature of the layer at the edge of plates differing from that in the interior. When the slurry is applied to the plate the layer is pinned at the edges so the layer thickness is thinner there and subject to a different drying and baking history. Data obtained for  $t < 40$  s (labelled A on the Figure) and  $t > 460$  s (labelled D) were therefore excluded from comparisons.

It is evident that stage A masks a rapid reduction in removal force caused by hydration following initial contact with solution. The  $F_w$  values measured after 60 s (stage B) lie in the range 100 – 150 N m<sup>-1</sup>, which is larger than that observed at pH 10 (Figure 6): the effect of pH is discussed in the next section. In stage B there is a slow decrease in  $F_w$  with time which in Figure 8(a) is masked by the scatter in the data: this feature is clearer in Figure 8(b), obtained at 50°C, and subsequent plots.

After 460 s at 20°C, there is a transition to a faster decay in  $F_w$  (labelled stage C): the transition time is labelled  $t_c$ . At 50°C, Figure 8(b),  $t_c \sim 220$  s and  $F_w$  decreases more quickly, with noticeably less scatter. The data could be fitted to an exponential decay expression with characteristic decay time,  $D$ ,  $\sim 125 \pm 3$  s, as well as less scatter.

The photographs in Figure 8 show that the transition is accompanied by a change in the amount of soil remaining on the substrate, with almost no residual material after  $t_c$ . These findings indicate that the adhesion of the soil to the substrate changes at  $t_c$ : the soil is still removed as a coherent layer, with cohesion within the soil (which may be decreasing due to the uptake of water) stronger than the adhesion to the substrate.

The B/C transition is more likely to arise from water penetrating through the soil (*i.e.* related to absorption and diffusion) rather than being due to ingress of water at the soil-

substrate interface. The latter would start as soon as there was contact with solution via the network of cracks in the layer.

Figure 8 confirms that temperature is an important parameter in cleaning of the CMS material, as Sinner's circle indicates. 50°C is a standard operating temperature in domestic dishwashers, and lies above the temperature estimated for the fat-rich phase in the CMS to become more fluid. The time taken for a 200 µm thick soil layer to reach 50°C after contacting the solution can be estimated by considering conduction through a slab of baked material with a thermal diffusivity of  $2 \times 10^{-7} \text{ m}^2/\text{s}$  (Rask, 1989). This gives a heating time of order 1 s, which is negligible. The initial  $F_w$  values are larger at 50°C than at 20°C (but subject to considerable scatter), which may be due to faster swelling. The B/C transition occurs earlier, which is consistent with faster diffusion, while the presence of mobile fat is likely to facilitate adhesive failure. A pseudo-exponential decay in stage C was not observed at 20° C. This may be because the solution was not in contact with the solution for long enough at this lower temperature.

#### *Effect of pH*

Many detergents are alkaline as this promotes swelling of proteins and hydrolysis of fats. The impact of pH on removing CMS layers was investigated primarily with water at pH 7 and aqueous NaOH solutions (pH 9 and 12) at 20 °C and at 50 °C.

Figure 9 shows that pH had little influence at 20 °C. The removal profiles are similar, with initial  $F_w$  values following hydration between 140 and 200  $\text{N m}^{-1}$ , followed by a slow linear decay. The B/C transition evident at pH 7 was not observed at pH 9 and occurred later, around 410 s, at pH 12. As a result the non-edge data were fitted to a simple linear trend: the decay rate was greatest at pH 9.

The removal profiles at 50°C at pH 9 and pH 12 in Figure 10 do not show the marked transition evident at 220 s at pH 7 (Figure 8(b)). Decay profiles measured at pH 6 and 8 were similar to those at pH 7 (Supplementary Figure S4). The initial  $F_w$  values are similar to those at 20 °C and the linear decay rates were faster at this higher temperature, at  $0.51 \pm 0.01 \text{ N m}^{-1} \text{ s}^{-1}$  (pH 7) and  $0.26 \pm 0.01 \text{ N m}^{-1} \text{ s}^{-1}$  at pH 9 and 12. Whereas  $F_w$  decayed almost exponentially in stage C at pH 7, the decay at pH 9 is close to linear



until  $t \sim 420$  s and at pH 12  $F_w$  does not decay strongly until around 300 s. The photograph provided as insets show a gradual change in residual soil on the substrate, which is consistent with the removal profiles.

The effect of alkali at 50°C is unexpected, as higher pH often accelerates cleaning of proteinaceous food soils (Morison and Thorpe, 2002; Fryer and Asteriadou, 2009), although some proteinaceous soils exhibit an optimal pH in alkaline cleaning (Mercade-Prieto *et al.*, 2006). In the absence of surfactants the cleaning agents active in this case are water (hydrating starch and proteins, dissolving soluble components), hydroxyl ions (indicative of pH) and  $\text{Na}^+$  counterions (both of which contribute to ionic strength/osmotic effects). Alkali conditions are known to cause unbaked protein layers to swell and promote erosion at the soil-solution interface (Tuladhar *et al.*, 2000; Christian and Fryer, 2006). Swelling would be expected to enhance transport of water to the substrate/soil interface and weaken the soil adhesion. Similarly, Otto *et al.* (2016) reported that unbaked starch deposits are expected to become more negatively charged at high pH and therefore be repelled from stainless steel surfaces which are similarly charged under these condition (isoelectric points typically pH 4-5 for 304 stainless steel (Lefevre *et al.*, 2009) and 5.1 for starch from wheat flowers (Kemp, 1936).

The results indicate that the hydroxyl ions are retarding the weakening of the adhesive interactions, which could be due to hydrolysis of the fats or inhibiting the mobility of the mobile fat phase, thereby retarding the access of water to the soil-substrate interface. The material at the interface is a complex mixture which has been subject to the oven temperature for 7 minutes (as a result of fast conduction through the steel). Further work is required to identify the components and processes active at this interface.

#### *Effect of surfactant*

The effect of 1 wt% surfactant was studied at pH 9 at 20°C and 50°C, representing standard dishwasher operating conditions. Figure 11 shows that the non-ionic (TX-100) and anionic (SDBS) surfactants gave no enhancement in removal, with similar changes in  $F_w$  over the test period (linear decay rates of  $0.14\text{--}0.15 \pm 0.01 \text{ N m}^{-1} \text{ s}^{-1}$ ). This is consistent with Figure 7 (pH 10 and 20 °C). Detry (2007, 2009) and Bobe (2007) demonstrated a beneficial impact of LAS-type surfactant in similar conditions on unburnt soils. This finding could be explained by the LAS acting via an

erosive/emulsification cleaning mechanism. Erosive cleaning has been shown by Gillham *et al.* (1999) and Chen *et al.* (2012) to be less effective for burnt materials due to their increased cohesive strengths and cross-linked polymeric structures relative to their unburnt counterparts.

In contrast the cationic agent, CTAB had immediate impact, giving almost exponential decay behaviour (initial decay rate  $0.42 \pm 0.01 \text{ N m}^{-1} \text{ s}^{-1}$ ), similar to pH 7 at 50°C, but without an evident B/C transition. The latter transition could have occurred at  $t < 40 \text{ s}$ , suggesting that either (i) CTAB aided the penetration of water through the soil to the substrate, or (ii) the reduction in adhesion was caused by ingress at the soil-substrate interface via the many cracks present in the soil layer. The photograph of the cleared region shows little residual material on the substrate, confirming that CTAB had promoted adhesive failure. The ability of CTAB to promote removal at room temperature brings immediate advantages in terms of energy consumption.

Figure 12 shows that all three surfactants promoted removal at 50°C at pH 9 compared to a simple alkaline solution. The removal profile for CTAB (Figure 12(a)) is similar to that at 20°C: fitting the data sets to simple exponential decay relationships gave  $D = 213 \pm 4 \text{ s}$  and  $238 \pm 5 \text{ s}$  at 20°C and 50°C, respectively. Temperature does not appear to have affected the CTAB mechanism. Determining the mechanism involved requires further work, but two possible explanations are (i) the cationic surfactant being attracted to the negatively charged starch-based moieties within the soil at pH 9; and (ii) the cationic surfactant having greater affinity for the stainless steel surface (which acquires a negative charge at pH 9), disrupting the adhesive bonding between the soil and the substrate at the interface and therefore lowering  $F_w$  even at room temperature. Hypothesis (ii) could be tested by using substrates with a different IEP but similar surface energy and heat conduction properties. In practice, hypothesis (ii) suggests that the effectiveness of a CTAB-based formulation would vary between surfaces.

The removal profiles for TX-100 and SDBS are both similar to that for water at pH 7 (Figure 8(b)), but with earlier B/C transition:  $t_c$  for TX-100 is markedly shorter, at approximately 80 s, while  $F_w$  decays more rapidly than with CTAB, with  $D = 139 \pm 3 \text{ s}$ . SDBS behaviour is very similar to the surfactant-free solution until  $t_c = 200 \text{ s}$ , after which  $F_w$  decays exponentially, unlike the alkaline solution, with  $D = 120 \pm 3 \text{ s}$ . The

final  $F_w$  values for TX-100 and SDBS (*i.e.* at  $t = 460$  s) are both smaller than that observed with CTAB.

The decay behaviours and decay rate parameters are summarised in Table 2. The existence of the B/C transition, faster decays and lower final  $F_w$  values all indicate that a different mechanism is involved in softening of the soil layer by the non-ionic and anionic surfactants.

The reason why TX-100 and SDBS promote behaviour observed at pH 7, essentially inhibiting the effect of higher pH, is now considered. SDBS will increase the solution ionic strength, while TX-100 will have little effect on charge. The observation that these surfactants are not effective at 20°C, when the fat phase is immobile, indicates that the mechanism is linked to the solubilising of fat globules present in the soil. Non-ionic surfactants are known to be effective at removing oily soils from synthetic fibres (Williams, 2007), whereas anionic surfactants are effective at removing (positively charged) particles. Since the fat prevents the ingress of water through the soil matrix, agents which promote the removal of this phase will enhance penetration of water and hydration at the soil-substrate interface. Removal of the oil phase will also affect the rheology of the hydrated soil, which will be manifested in the cohesive contribution to the force measured by the millimanipulation blade. This mechanism would not be directly affected by the nature of the substrate to the same degree as that promoted by CTAB. The substrate would have an indirect effect in terms of wetting characteristics towards components in the soil, heat transfer etc. and therefore microstructure of the fouling layer at the soil-substrate interface (see Magens *et al.*, 2017).

These results demonstrate how the different agents effect cleaning, reducing the strength of the soil at the soil-substrate interface via different mechanisms. The same length of time may be required to remove the CMS layers studied here from a stainless steel surface, but knowledge of the mechanisms – whether ingress or penetration – allows one to gauge whether or not the agent will give similar efficacy for other soils on different substrates.

The cleaning mechanism and behaviour is ultimately determined by the nature and microstructure of the soil. For example, Ali *et al.* (2015a) studied the cleaning of polymerised lard soil layers on stainless steel and reported that solutions of TX-100 and LAS at pH 10.4-11 promoted solution ingress and soil detachment at the soil-substrate

interface, while CTAB promoted penetration through the soil layer (rather than promoting ingress as observed in this work). These differences illustrate how, like coatings to prevent deposition and fouling, detergent solutions need to be matched to the soil.

## Conclusions

The millimanipulation technique has been extended to allow the forces at the soil-substrate interface to be measured whilst being immersed and soaked in cleaning solutions in real time. The complex model food soil tested comprised burnt fats, starch and proteins in a cracked layer on stainless steel: it was not possible to prepare uniform soil layers. The adhesion forces decreased noticeably on hydration.

The soils exhibited cohesive or adhesive failure during removal, depending on the cleaning solution chemistry. Temperature had a uniformly beneficial effect on cleaning, with water at pH 7 at 50°C exhibiting a transition between cohesive and adhesive failure after an initial soaking period. The length of this initial soaking period was reduced when TX-100 or SDBS was present. This behaviour is attributed to the fat in the soil being mobile at 50°C. CTAB, the cationic surfactant, promoted adhesive failure at 20°C and 50°C, indicating that its action involved a different mechanism.

The pH of the solution impacts had little influence at 20 °C. At 50 °C, high pH gave slower cleaning than at pH 6-8, even though alkaline conditions are expected to promote swelling and weakening of proteins in the deposit. All three surfactants studied promoted removal at high pH, with TX-100 giving greatest reduction in soil strength. The results provide quantitative evidence that different cleaning mechanisms are promoted by the different cleaning agents, and allow their role in Sinner's circle to be quantified in terms of the extent and rate of change of the rheology of the soil at the soil-substrate interface.

## Acknowledgements

607 An iCASE PhD studentship for GLC from EPSRC and Procter & Gamble is gratefully  
608 acknowledged, as are helpful conversations with Ole Mathis Mogens.

609

#### 610 **Open Data**

611 The data presented in this study are available from the University of Cambridge's  
612 Apollo data repository at doi 10.17863/CAM.26373.

## 613    **References**

- 614    Akhtar, N., Bowen, J., Asteriadou, K., Robbins, P. T., Zhang, Z., Fryer P. J. (2010)  
615         Matching the nano- to the meso-scale: Measuring deposit–surface interactions  
616         with atomic force microscopy and micromanipulation, *Food and Bioproducts*  
617         Processing, 88, 341–348.
- 618    Ali, A. (2015) PhD: Understanding the cleaning of greasy polymerised food soils.  
619         University of Cambridge, Cambridge.
- 620    Ali, A., Alam, Z., Ward, G., Wilson, D. I. (2015a) Using the fluid dynamic gauging  
621         device to understand the cleaning of baked lard soiling layers. *J. Surfactants*  
622         Detergents, 18, 933-947.
- 623    Ali, A., de’Ath, D., Gibson, D., Parkin, J., Ward, G., Alam, Z. and Wilson, D.I. (2015b)  
624         Development of a millimanipulation device to quantify the strength of food  
625         fouling deposits, *Food Bioproducts Proc.*, 93, 265-258
- 626    Asteriadou, K., Othman, A.M., Goode, K., Fryer, P.. (2009) Improving cleaning of  
627         industrial heat induced food and beverages deposits: A scientific approach to  
628         practice. *Heating Exchanger and Fouling Conference*. 158-164
- 629    Ashokkumar, S., Adler-Nissen, J., 2011. Evaluating non-stick properties of different  
630         surface materials for contact frying. *J. Food Eng.* 105, 537–544.
- 631    Basso, M., Simonato, M., Furlanetto, R., De Nardo L., (2017) Study of chemical  
632         environments for washing and descaling of food processing appliances: An  
633         insight in commercial cleaning products. *J. Ind. Eng. Chem.*, 53, 23-36.
- 634    Bishop, A. 1997, *Cleaning in the Food Industry*, Reprinted by permission of Wesmar  
635         Company Inc. from *Basic Principles of Sanitation*.
- 636    Bobe, U., Hofmann, J., Sommer, K., Beck, U., Reiners, G., (2007) Adhesion - where  
637         cleaning starts, *Trends Food Sci. Technol.*, 18, 36-39.
- 638    Castner, D. G., Ratner, B. D. (2002) Biomedical surface science: foundations to  
639         frontiers. *Surf. Sci.*, 500, 28-60.
- 640    Chen, X., Fickak, A., Hatfield, E. (2012) Influence of run time and aging on fouling  
641         and cleaning of whey protein deposits on heat exchanger surface. *J. Food Res.*,  
642         1, 212-224.
- 643    Chew, J.Y.M., Paterson, W.R. and Wilson, D.I. (2004) Dynamic gauging for measuring  
644         the strength of soft deposits, *J. Food Eng.* 65(2), 175-187.
- 645    Christian, G. K., Fryer, P. J. (2006) The effect of pulsing cleaning chemicals on the  
646         cleaning of whey protein deposits, *Food Bioproducts Proc.*, 84, 320-328.

- 647 Detry J. G., Rouxhet, P. G., Boulange-Petermann, L., Deroanne, C., Sindic, M., (2007)  
 648 Cleanability assessment of model solid surfaces with a radial-flow cell. *Colloids*  
 649 *Surf. A: Physicochem. Eng. Aspects*, 302, 540-548.
- 650 Detry, J. G., Deroanne, C., Sindic, M. (2009) Hydrodynamic systems for assessing  
 651 surface fouling, soil adherence and cleaning in laboratory installations,  
 652 *Biotechnol. Agron. Soc. Environ.* 13, 427-439
- 653 Din, R. A., Bird, M. R. (1996) The effect of water on removing starch deposits formed  
 654 during baking, *Proc. 2nd European Conference for Young Researchers in*  
 655 *Chemical Engineering*, Leeds, UK, 1, 187–189.
- 656 Dunstan, T. S., Fletcher, P. D. I., (2014) The removal of thermally aged films of  
 657 triacylglycerides by surfactant solutions. *J. Surfact. Deterg.*, 17, 899-910.
- 658 Fryer, P. J., Asteriadou, K. (2009) A prototype cleaning map: a classification of  
 659 industrial cleaning processes. *Trends in Food Science & Technology*, 20, 225–  
 660 262.
- 661 Gordon, P.W., Brooker, A.D.M., Chew, Y.M.J., Wilson, D.I., York, D.W. (2010)  
 662 Studies into the swelling of gelatine films using a scanning fluid dynamic gauge,  
 663 *Food & Bioprod. Proc.*, 88, 357-364
- 664 Gillham, C. R., Fryer, P. J., Hasting, A. P. M. and Wilson, D. I. (1999) Cleaning-in-  
 665 place of whey protein fouling deposits: Mechanisms controlling cleaning,  
 666 *Food Bioprod. Proc.*, 77, 127-136.
- 667 Gillham, C.R., Fryer, P.J., Hasting, A.P.M. and Wilson, D.I. (2000) Enhanced cleaning  
 668 of whey protein fouling deposits using pulsed flows, *J. Food Engineering*, 46(3),  
 669 199-209.
- 670 Hauser, G. (2008) *Hygiene gerechte Apparate und Anlagen: für die Lebensmittel-,*  
 671 *Pharma- und Kosmetikindustrie*. Wiley-VCH, Weinheim
- 672 Israelachvili, J. (2011) *Intermolecular and Surface Forces*, Elsevier. Ch. 13, 17.
- 673 Jennings, W. G., (1965) Theory and practice of hard-surface cleaning, *Adv. Food Res.*,  
 674 14, 325-458
- 675 Jonhed, A., Andersson, C., Jarnstrom, L. (2008) Effects of film forming and  
 676 hydrophobic properties of starches on surface sized packaging paper. *Packaging*  
 677 *Technol. Sci.*, 21, 123-135.
- 678 Jurado-Alameda, E., Herrera-Márquez, O., Martínez-Gallegos, J. F., Vicaria, J. M.  
 679 (2015) Starch-soiled stainless steel cleaning using surfactants and  $\alpha$ -amylase, *J.*  
 680 *Food Eng.* 160, 56-64.

- 681 Kemp, I. (1936) The surface analysis of particles of certain wheat flours. Trans. Faraday  
682 Soc., 32, 837-843.
- 683 Kumar, A., Staedler, T., Jiang, X. (2013) Role of relative size of asperities and adhering  
684 particles on the adhesion force. J. Colloid Interface Sci. 409, 211-218.
- 685 LaMarche, C., Leadley, S., Liu, P., Kellogg, K.M., Hrenya, C.M., (2017) Method  
686 of quantifying surface roughness for accurate adhesive force predictions,  
687 Chem. Eng. Sci, 158, 140-153.
- 688 Lee, W.P., Routh, A.F. (2004) Why do drying films crack? Langmuir, 20, 9885-9888.
- 689 Lefèvre, G., Čerović, L, Milonjić, S., Fédoroff, M., Finne, J., Jaubertie, A. (2009)  
690 Determination of isoelectric points of metals and metallic alloys by adhesion of  
691 latex particles, J. Colloid Interface Sci, 337, 449–455.
- 692 Lelièvre, C., Legentilhomme, P., Gaucher, C., Legrand, J., Faille, C., and Bénézech,  
693 T. (2002) Cleaning in place: Effect of local shear stress variation on bacterial  
694 removal from stainless steel equipment, Chem. Eng. Sci., 57, 1287–1287.
- 695 Lelieveld, H.L.M., Mostert, M.S., Holah, J. (2005) Handbook of hygiene control in the  
696 food industry. EHEDG, Cambridge, UK, publ. Woodhead, 192 – 208.
- 697 Li, H., Koutzenko, B., Chen, X.D., Jentet, R., Mercadé-Prieto, R. (2015) Cleaning  
698 beyond whey protein gels: Egg white, *Food Bioproduct Proc.*, 93, 249-255.
- 699 Liu, W., Christian, G. K., Zhang, Z., Fryer, P.J. (2002) Development and use of a  
700 micromanipulation technique for measuring the force required to disrupt and  
701 remove fouling deposits. Food Bioprod. Proc. 80, 286-291.
- 702 Liu, W., Fryer, P.J., Zhang, Z., Zhao, Q., Liu, Y. (2006) Identification of cohesive and  
703 adhesive effects in the cleaning of food fouling deposits. Innovative Food  
704 Science Emerging Tech., 7, 263-269.
- 705 Magens, O.M., Liu, Y., Hofmans, J.F.A., Nelissen, J.A., Wilson, D.I. (2017)  
706 Adhesion and cleaning of foods with complex structure: Effect of oil content  
707 and fluoropolymer coating characteristics on the detachment of cake from  
708 baking surfaces, J. Food Eng., 197, 48-59.
- 709 Mashmouhy, H., Zhang, Z., Thomas, C.R., (1998) Micromanipulation measurement  
710 of the mechanical properties of baker's yeast cells, Biotechnology Techniques,  
711 12, 925–929.



- 712 Mauermann, M., Eschenhagen, U., Bley T. H., Majschak, J.-P. (2009) Surface  
713 modifications e Application potential for the reduction of cleaning costs in the  
714 food processing industry, Trends Food Science & Technology, 20, 8-15
- 715 Mercadé-Prieto, R., Falconer, R.J., Paterson, W.R., Wilson, D.I. (2006) Probing the  
716 mechanisms limiting dissolution of whey protein gels during cleaning, 84, 311-  
717 319
- 718 Moeller, R. S., Nirschl, H. (2017) Adhesion and cleanability of surfaces in the baker's  
719 trade, J. Food Eng., 194, 99-108.
- 720 Morison, K. R., Thorpe, R. J. (2002) Spinning disc cleaning of skimmed milk and whey  
721 protein deposits. Food Bioprod. Proc, 80, 319-325.
- 722 Otto, C., Zahn, S., Hauschild, M., Babick, F., Rohm, H. (2016) Comparative cleaning  
723 tests with modified protein and starch residues, J. Food Eng. 178, 145-150.
- 724 Palmisano, P., Hernandez, S. P., Hussaina, M., Finoa, D., Russoa, N. (2011) A new  
725 concept for a self-cleaning household oven, Chem. Eng. J, 176–177, 253–259.
- 726 Pérez-Mohedano, R., Letzelter, N., Bakalis, S. (2016) Swelling and hydration studies  
727 on egg yolk samples via scanning fluid dynamic gauge and gravimetric tests. J.  
728 Food Eng., 169, 101-113.
- 729 Pongsawasdi, P., Murakami, S. (2010) *Carbohydrases in detergents*, Nova Science  
730 Publishers, 71-95.
- 731 Previdello B. A. F., Carvalho F. R. D., Tessaro A. L., Souza V. R. D., and Hioka N.,  
732 (2006). The pKa of acid-base indicators and the influence of colloidal systems.  
733 Química Nova, 29, 600–606.
- 734 Prochaska, K., Kędziora, P., Thanh, J.L., Lewandowicz, G. (2007) Surface activity of  
735 commercial food grade modified starches. Coll. Surf. B. Biointerfaces, 60, 187-  
736 194.
- 737 Rask, C. (1989) Thermal properties of dough and bakery products: A review of  
738 published data, J. Food Eng, 9, 167-193.
- 739 Rosa, F., Roviada, E., Graziosi, S., Giudici, P., Guarnaschelli, C., and Bongini, D. (2012)  
740 Dishwasher history and its role in modern design, Third IEEE History of  
741 Electro-technology conference 'The Origins of Electrotechnologies', Pavia,  
742 Italy.
- 743 Rosen, M. J., Kunjappu, J.T, 2012, *Surfactants and Interfacial Phenomena*, John  
744 Wiley & Sons Inc., New Jersey, 2012.

- 745 Ruiz C. C., Molina-Bolivar J. A., Aguiar J., MacIsaac G., Moroze S., and Palepu R.,  
746 (2001). Thermodynamic and structural studies of Triton X-100 micelles in  
747 ethylene glycol-water mixed solvents. *Langmuir*, 17, 6831–6840.
- 748 Saikhwan, P., Mercadé-Prieto R., Chew , Y.M.J., Gunasekaran, S., Paterson, W.R. and  
749 Wilson, D.I. (2010) Swelling and dissolution in cleaning of whey protein gels,  
750 *Food & Bioproducts Proc.*, 88, 375–383.
- 751 Sanz J., Lombraña J. I., and Luís A.de, (2003). Ultraviolet-H<sub>2</sub>O<sub>2</sub> oxidation of  
752 surfactants. *Environmental Chemistry Letters*, 1, 32–37.
- 753 Showell, M., 2005, Part D: Formulation, *Handbook of Detergents*, Boca Raton, Florida,  
754 CRC Press, 158-163.
- 755 Stanga, M., (2010) *Sanitation: Cleaning and Disinfection in the Food Industry*.  
756 Wiley VCH, Weinheim.
- 757 Tuladhar, T. R., Paterson, W. R., Wilson, D. I. (2002) Thermal conductivity of whey  
758 protein film undergoing swelling: measurement by dynamic gauging, *Food*  
759 *Bioprod. Proc.*, 80, 332-339.
- 760 Williams, J, (2007), Formulation of Carpet Cleaners, *Handbook for Cleaning /*  
761 *Decontamination of Surfaces*, 1, 103-123.
- 762

763 **Nomenclature**

764 **Roman**

765	$D$	characteristic decay time (s)
766	$h$	height of blade above substrate (m)
767	$F_w$	removal force per unit width ( $\text{N m}^{-1}$ )
768	$R_q$	roughness parameter (m)
769	$V$	velocity of blade ( $\text{m s}^{-1}$ )
770	$t$	time (s)
771	$x$	distance travelled by blade (m)
772	$t_c$	transition point in decay behaviour (s)
773	$t_{\text{soak}}$	soaking time (s)

774

775 **Greek**

776	$\gamma^{\text{LS}}$	surface energy between liquid and solid phases ( $\text{J m}^{-2}$ )
777	$\delta$	soil layer thickness (m)

778

779 **Acronyms**

780	AFM	atomic force microscopy
781	CIP	clean in place
782	CMS	complex model soil
783	CTAB	hexadecyltrimethylammonium bromide
784	FDG	fluid dynamic gauging
785	LAS	linear alkyl sulfonate
786	MM3	millimanipulation mk 3
787	MM3-Flow	millimanipulation mk 3 with circulation system
788	SDBS	sodium dodecyl benzene sulfonate
789	SS	stainless steel
790	TX-100	t-octylphenoxypolyethoxyethanol

791

## Figure Captions

Figure 1. Photographs of  $\delta = 300 \mu\text{m}$  CMS layer on  $50 \times 50 \text{ mm}$  316 stainless steel plate (a) before drying, and (b) after baking for 7 min at  $204^\circ\text{C}$ ; (c) Binary image of (b) for calculating area of cracked soil; (d) image (b) with gridlines used for calculating crack distribution.

Figure 2: Side view of the millimanipulation device with flow chamber fitted. Labels: A, Perspex viewing wall; B, blade; C, force transducer; D, counterweight; E, sample mounting station; I, solution inlet; O, solution outlet. Dashed arrow indicates direction of sample motion.

Figure 3: Conductivity of solution leaving test chamber before and after addition of NaOH solution to the reservoir at  $t = 10 \text{ min}$ . Data from three repeats. The grey area indicates the section plotted in the inset. Solution flow rate  $100 \text{ mL min}^{-1}$ .

Figure 4: Effect of contact with cleaning solution on residual soil on substrate. (a) schematic of testing regions; (b) photograph of plate after testing with (conditions for B: 5 minutes soaking in 1 wt% SDBS solution at room temperature). All dimension in mm.

Figure 5: Side-on view of the removal of an example of (a) dry soil and (b) soil immersed in surfactant solution. Identical CMS soils with differences in lighting conditions and submersion in solution causing apparent colour differences.

Figure 6:  $F_w$  profiles (a) before (region A in Figure 4) and (b) after soaking in 1wt% SDBS solution at pH 10 at room temperature (region B in Figure 4). The transducer range sets a limit on  $F_w$  of  $430 \text{ N m}^{-1}$  which is evident in (a). Legend denotes start time of the test.

Figure 7: Effect of soaking at pH 10 at room temperature with (solid circles) and without 1 wt% SDBS (open circles). Insert: full data containing 60 min data points. Error bars show time scale of averaged data points.

Figure 8: Effect of temperature on removal force following contact with pH 7 solution at  $t = 0$  at (a)  $20^\circ\text{C}$ ; (b)  $50^\circ\text{C}$ . Dashed vertical lines mark initial and final regions

822 subject to edge effects, repeated in subsequent plots. Dot-dashed lines mark the  
823 transition in decay behaviour at  $t_c$ : photograph in (b) shows the plate after  
824 testing. Solid line in in (b) shows fit to exponential decay  $F_w = 920 \exp[-t'/125]$ .

825 Figure 9: Effect of pH on removal profiles at 20°C. Solid loci show linear regression to  
826 data in the range  $50 < t < 350$  s. Vertical dashed lines mark initial and final  
827 regions subject to edge effects.

828 Figure 10: Effect of pH on removal profiles at 50 °C. (a) pH 9, (b) pH 12: pH 7 data  
829 given in Figure 8(b). Vertical dashed lines mark region A and D (edge effects).  
830 Dot-dashed lines marks B/C transition observed at pH 7 at 220 s. Photographs  
831 show substrate after testing.

832 Figure 11: Effect of surfactant on removal force at 20 °C. Soil is contacted with pH 9  
833 solution at  $t = 0$ . Lines show linear regression to data in the range  $50 < t < 350$   
834 s. Vertical dashed lines mark initial and final regions subject to edge effects.  
835 Photograph shows cleared region after testing with CTAB solution.

836 Figure 12: Effect of 1 wt% surfactant on removal profiles at pH 9 and 50°C. (a) CTAB,  
837 (b) TX-100, (c) SDBS solution. Grey symbols show profile obtained without  
838 surfactant (Figure 10(a)). Vertical dashed lines mark initial and final regions  
839 subject to edge effects. Vertical dot-dash line marks B/C transition. Solid lines  
840 show fit of data in stage C to a simple exponential decay.

841

842

### Supplementary Figure Captions

Figure S1: Schematic of sample spreading device. (a) front view; (b) section through plane AA'; (c) photograph. M indicates micrometers used to set the substrate-blade gap. Dimensions are in mm.

Figure S2: DSC thermograms of (a) fresh and (b) fresh, dried and burnt CMS. Temperature ramped from -20 to 100 °C at 5 K min<sup>-1</sup> twice, as shown by inset in (a). Fresh; black – scan 1, grey – scan 2. Dried; blue – scan 1, purple – scan 2. Burnt; orange – scan 1, red – scan 2.

Figure S3: Shear viscosity of fat component of CMS (40 % emulsion of fat in water). Apparent viscosity measured at apparent shear rate of 0.1 s<sup>-1</sup>. Open symbols indicate data with significant normal stress differences, indicating strongly non-Newtonian behaviour. Inset shows the shear rate dependency at 22°C: below 0.1 s<sup>-1</sup> the gradient is close to -1, associated with yield stress behaviour.

Figure S4: Effect of pH on removal profiles at 50 °C. Blue pH 6 D ~ 230, Grey pH 8 D ~ 220. Vertical dashed lines mark region A and D (edge effects). Dot-dashed line marks B/C transition, observed at 200 s for both pH 6 and 8. Image shows an example of the substrate after testing. Note:  $F_w$  in section B is lower than that measured at pH 7 for a different CMS batch (Figure 8(b)).

863 **Tables**

864 Table 1: Model soil composition

Component	mass fraction	nature	Supplier/source
	wet basis		
fat	0.18	mixture of saturated and unsaturated fats	margarine blend 'I can't believe it's not butter™', whole milk
protein	0.057	milk protein	whole milk, Kraft cheese powder pasta (cooked)
carbohydrate	0.240	durum wheat starch	pasta (cooked)
salt	0.003	NaCl, dissolved	Kraft cheese powder
water	0.52	deionised water	pasta (cooked), whole milk

865

866

867

868 Table 2: Summary of rate of change of adhesion forces over 500 s testing. Values in  
869 parentheses are the uncertainty in the parameters, based on one standard  
870 deviation.

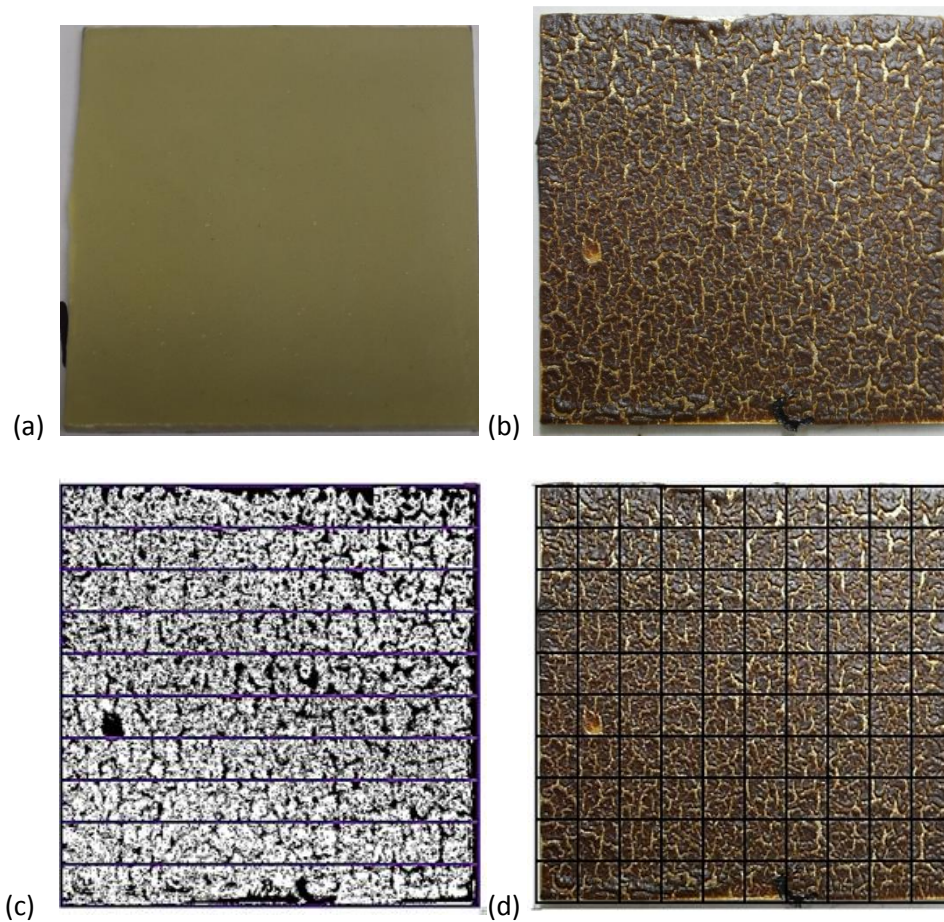
pH	surfactant (1 wt%)	$t_c$		linear decay rate		$D$	
		/s		$/\text{N m}^{-1}\text{s}^{-1}$		/s	
		20°C	50°C	20°C	50°C	20°C	50°C
7		-	220	0.06±0.007	0.51±0.01	-	125±3
9		-	220	0.15±0.02	0.26±0.01	-	-
12		-	300	0.11±0.01	0.26±0.01	-	-
9	SDBS	-	200	0.14±0.01	0.41±0.01	-	120±3
9	CTAB	40	40	0.42±0.01	-	213±4	238±5
9	TX-100	-	80	0.15±0.01	-	-	139±3

871

872



873 **Figures**



879 Figure 1. Photographs of  $\delta = 300 \mu\text{m}$  CMS layer on  $50 \times 50 \text{ mm}$  316 stainless steel  
 880 plate (a) before drying, and (b) after baking for 7 min at  $204^\circ\text{C}$ ; (c) Binary  
 881 image of (b) for calculating area of cracked soil; (d) image (b) with gridlines  
 882 used for calculating crack distribution.

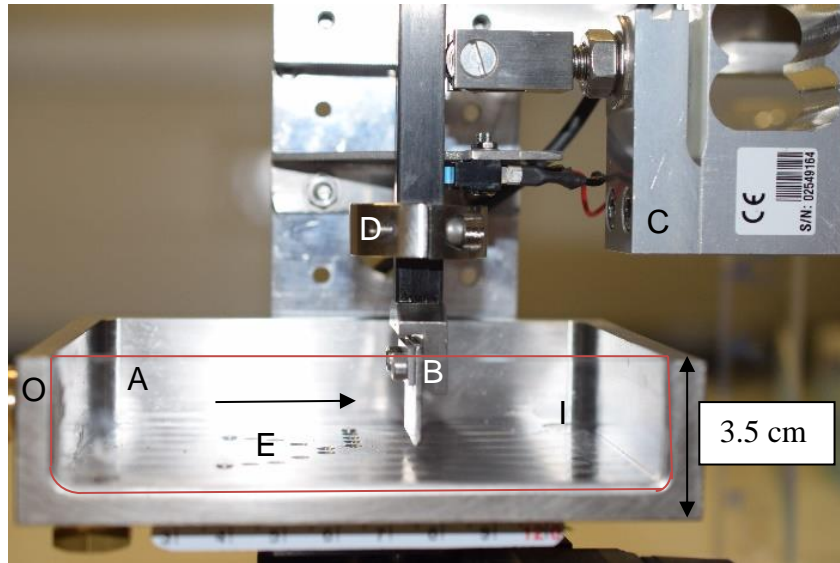


Figure 2: Side view of the millimanipulation device with flow chamber fitted. Labels: A, Perspex viewing wall outlined in red; B, blade; C, force transducer; D, counterweight; E, sample mounting station; I, solution inlet; O, solution outlet. Dashed arrow indicates direction of sample motion.

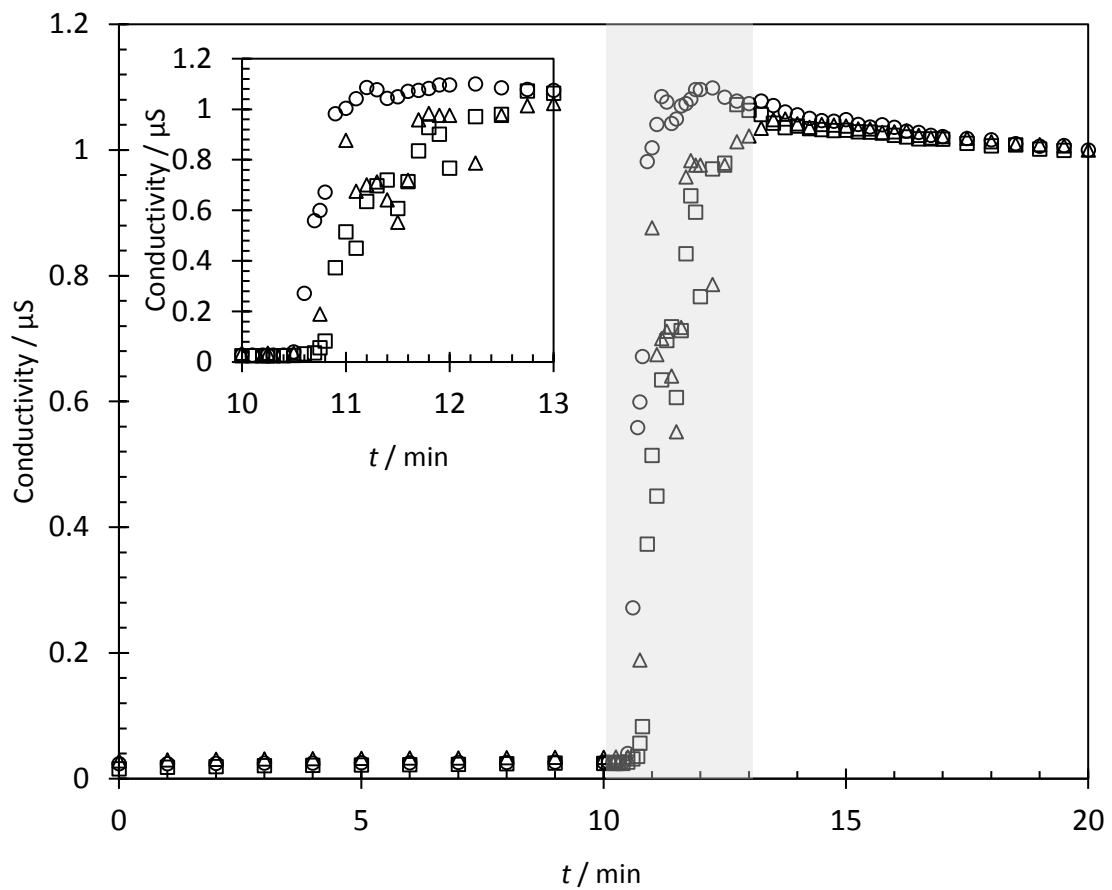


Figure 3: Conductivity of solution leaving test chamber before and after addition of NaOH solution to the reservoir at  $t = 10$  min. Data from three repeats. The grey area indicates the section plotted in the inset. Solution flow rate 100 mL  $\text{min}^{-1}$ .

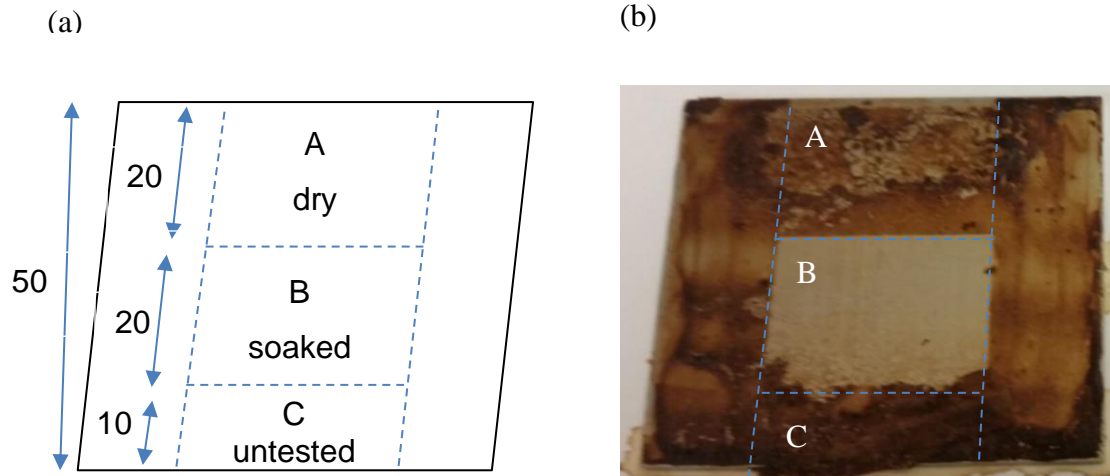


Figure 4: Effect of contact with cleaning solution on residual soil on substrate. (a) schematic of testing regions; (b) photograph of plate after testing with (conditions for B: 5 minutes soaking in 1 wt% SDBS solution at room temperature). All dimension in mm. Blade clearance: 50  $\mu\text{m}$ .

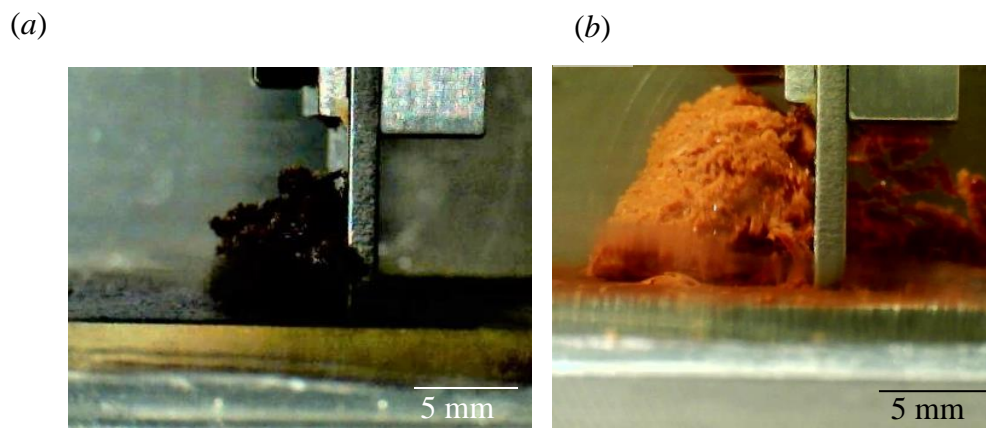
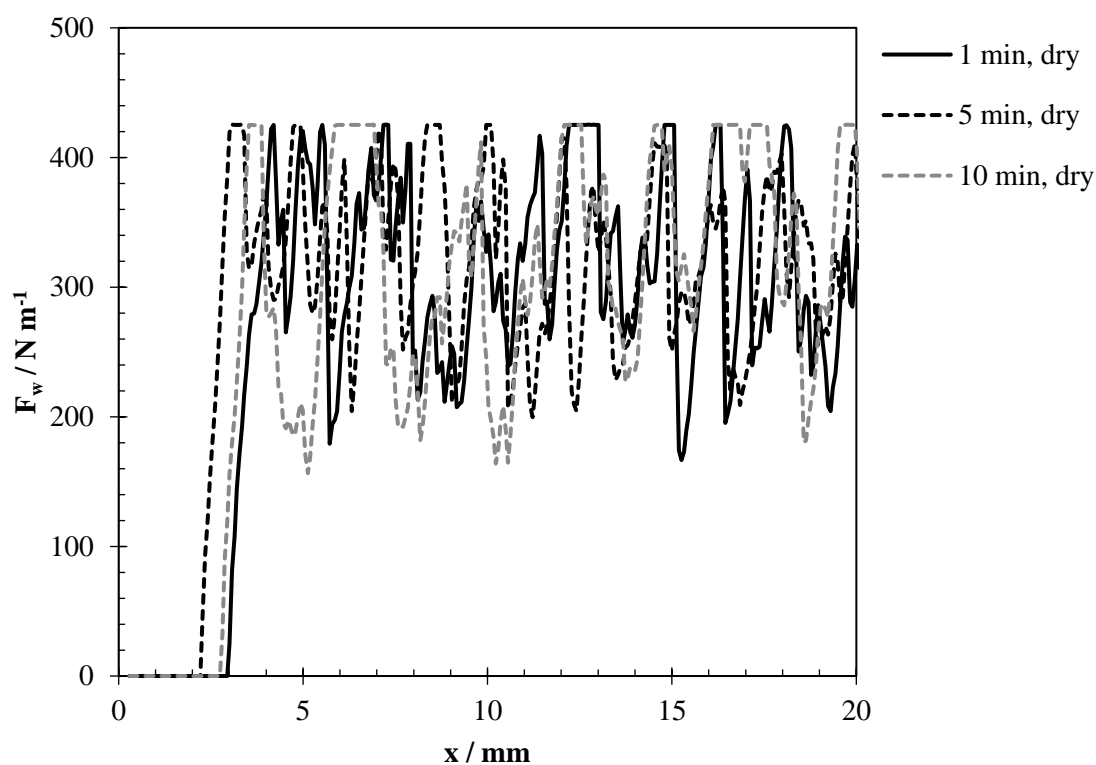


Figure 5: Side-on view of the removal of an example of (a) dry soil and (b) soil immersed in surfactant solution. Identical CMS soils with differences in lighting conditions and submersion in solution causing apparent colour differences.

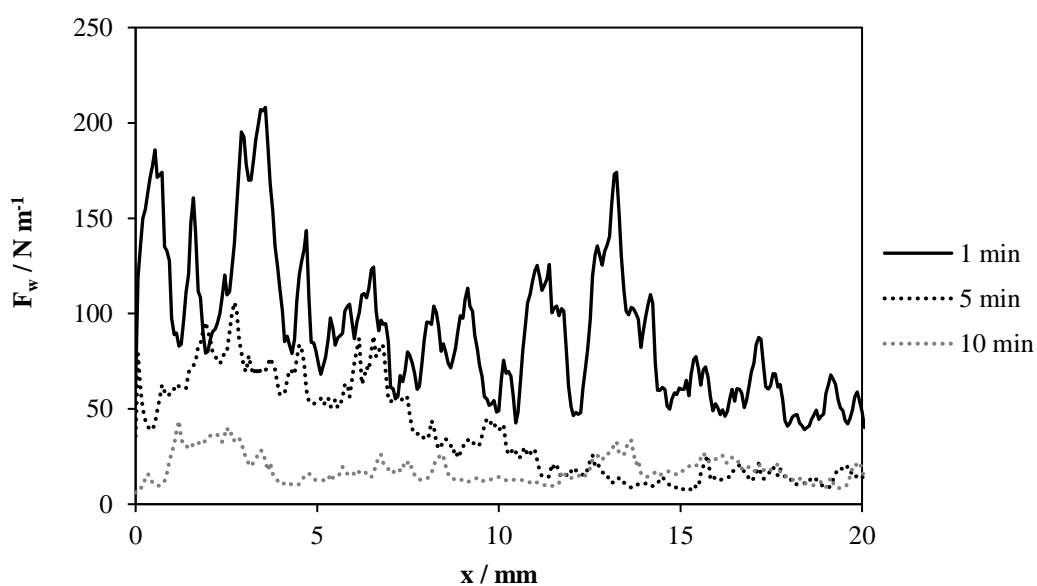
911

(a)



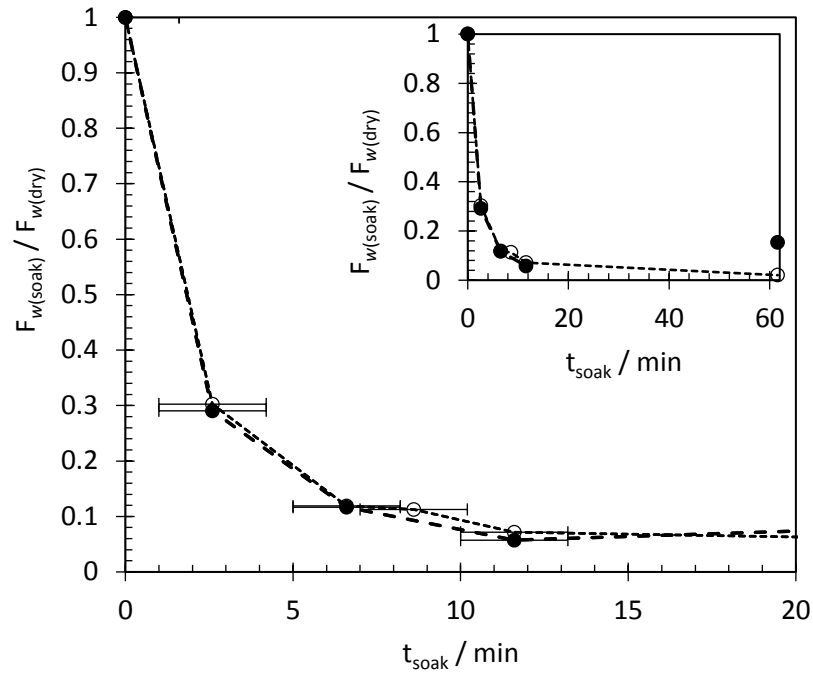
912

(b)



913

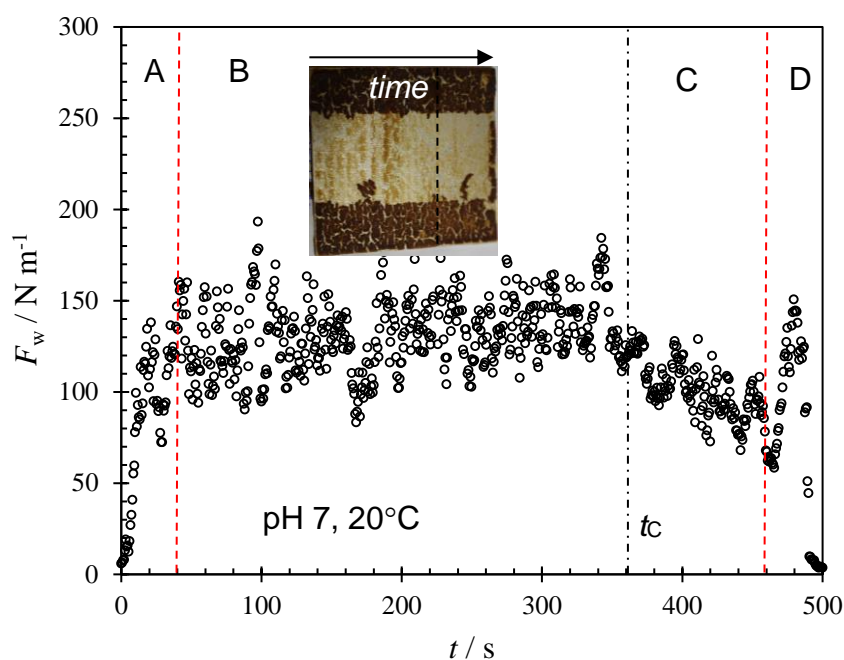
914 Figure 6.  $F_w$  profiles (a) before (region A in Figure 4) and (b) after soaking in 1wt%  
 915 SDBS solution at pH 10 at room temperature (region B in Figure 4). The  
 916 transducer range sets a limit on  $F_w$  of  $430 \text{ N m}^{-1}$  which is evident in (a). Legend  
 917 denotes start time of the test.



918

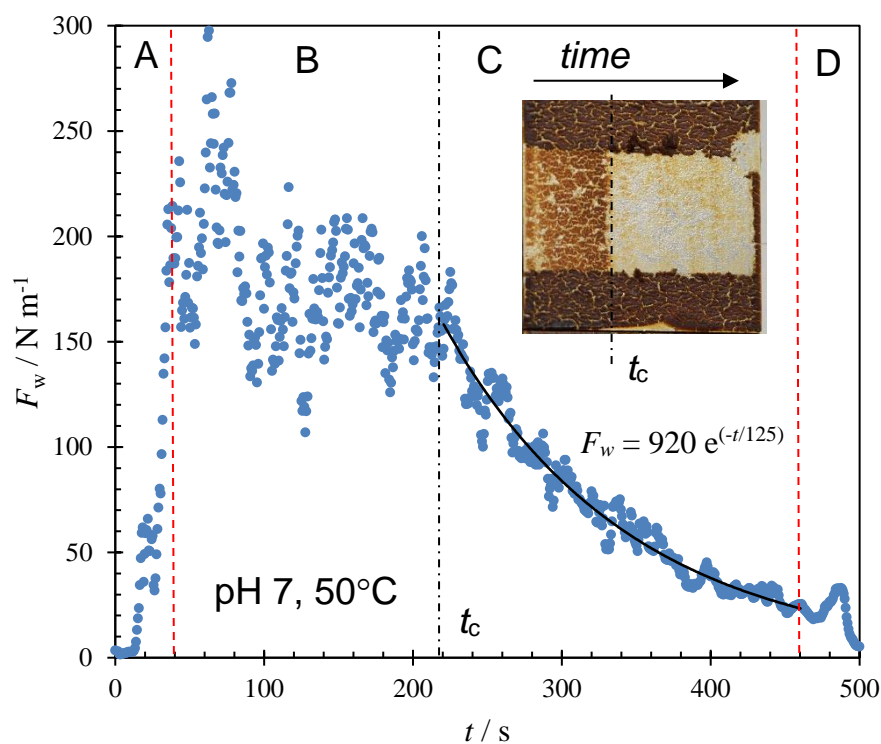
919 Figure 7: Effect of soaking at pH 10 at room temperature with (solid circles) and  
 920 without 1 wt.% SDBS (open circles). Insert: full data containing 60 min data  
 921 points. Error bars show time scale of averaged data points.

922 (a)



923

924 (b)



925

926 Figure 8: Effect of temperature on removal force following contact with pH 7 solution  
 927 at  $t=0$  at (a) 20°C; (b) 50 °C. Dashed vertical lines mark initial and final regions  
 928 subject to edge effects, repeated in subsequent plots. Dot-dashed lines mark the  
 929 transition in decay behaviour at  $t_c$ : photograph in (b) shows the plate after  
 930 testing. Solid line in in (b) shows fit to exponential decay  $F_w = 920 \exp[-t'/125]$ .

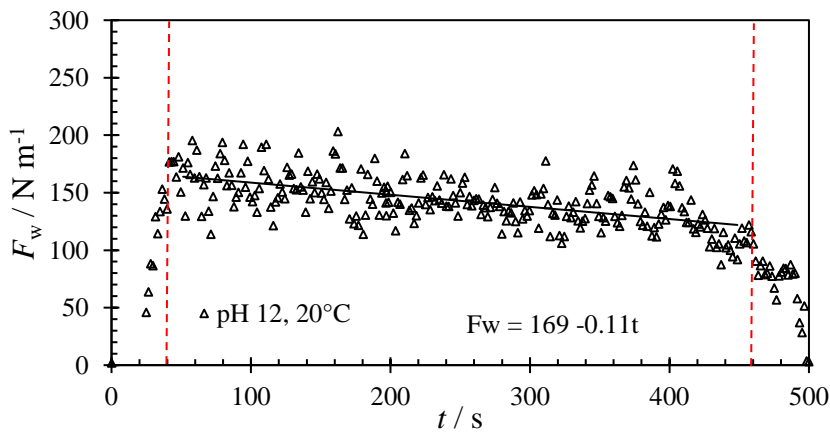
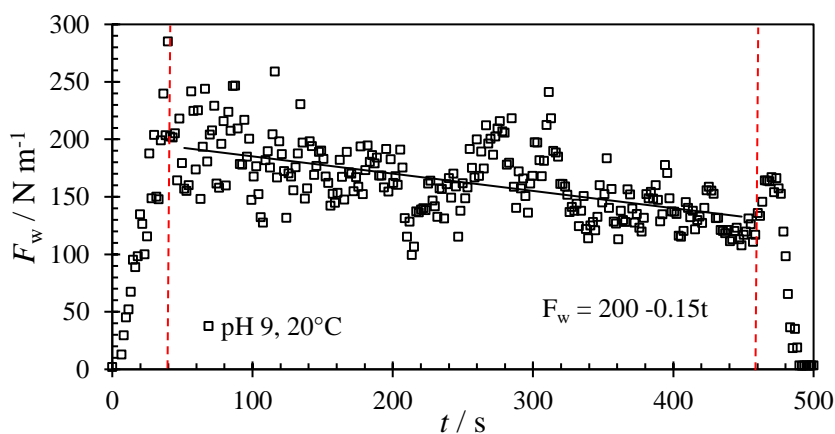
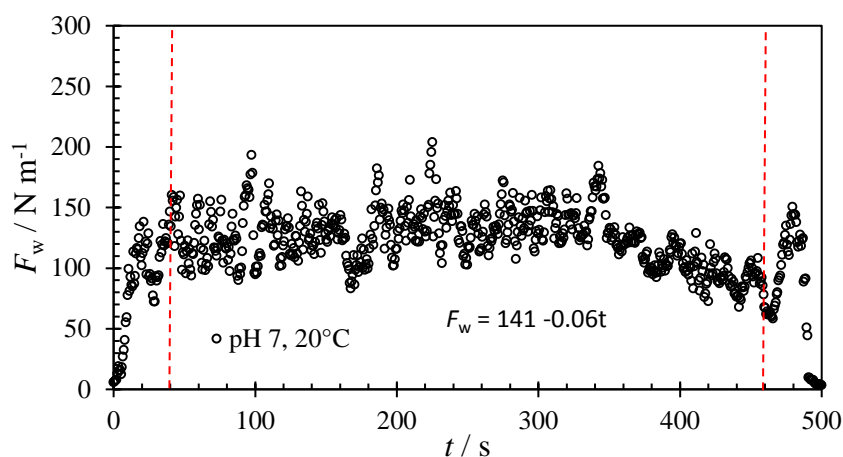
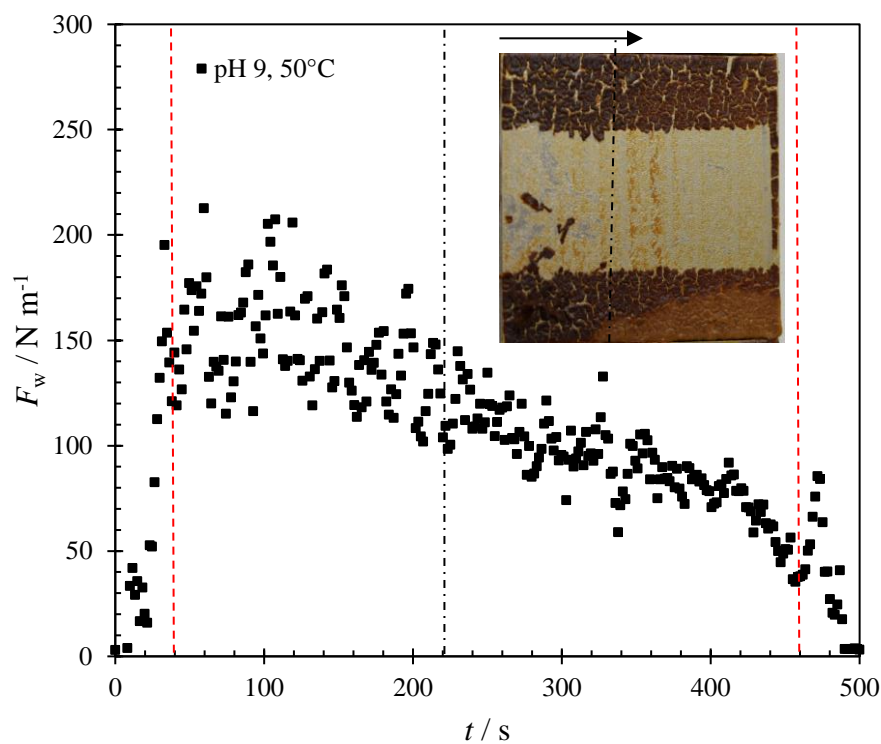


Figure 9: Effect of pH on removal profiles at 20°C. Solid loci show linear regression to data in the range  $50 < t < 350$  s. Vertical dashed lines mark initial and final regions subject to edge effects.

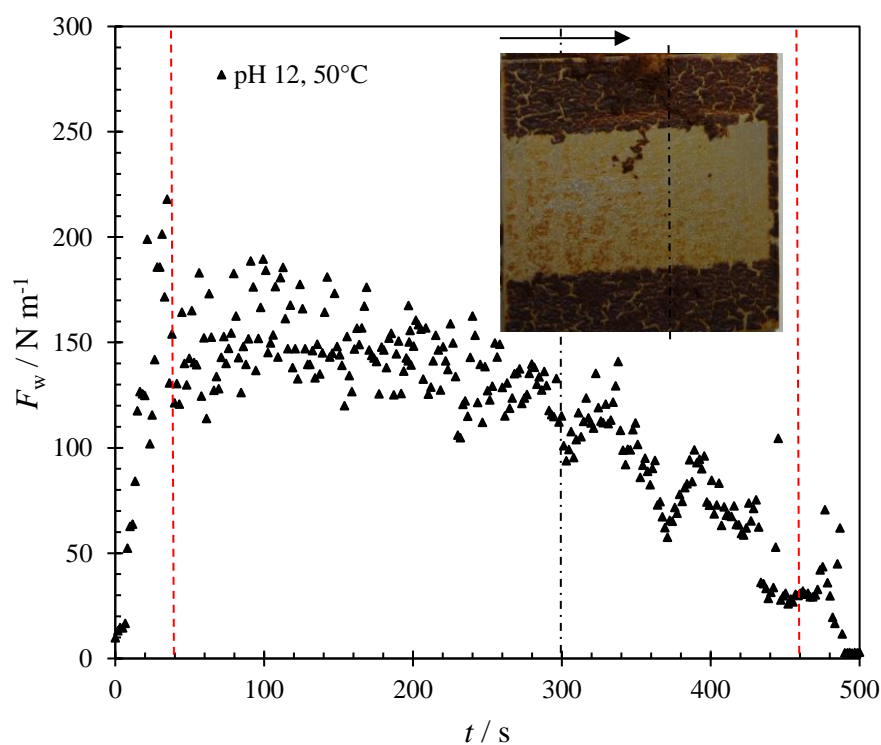


938 (a)



939

940 (b)



941

942 Figure 10: Effect of pH on removal profiles at 50 °C. (a) pH 9, (b) pH 12: pH 7 data  
 943 given in Figure 8(b). Vertical dashed lines mark region A and D (edge effects).  
 944 Dot-dashed lines marks B/C transition observed at pH 7 at 220 s. Photographs  
 945 show substrate after testing.

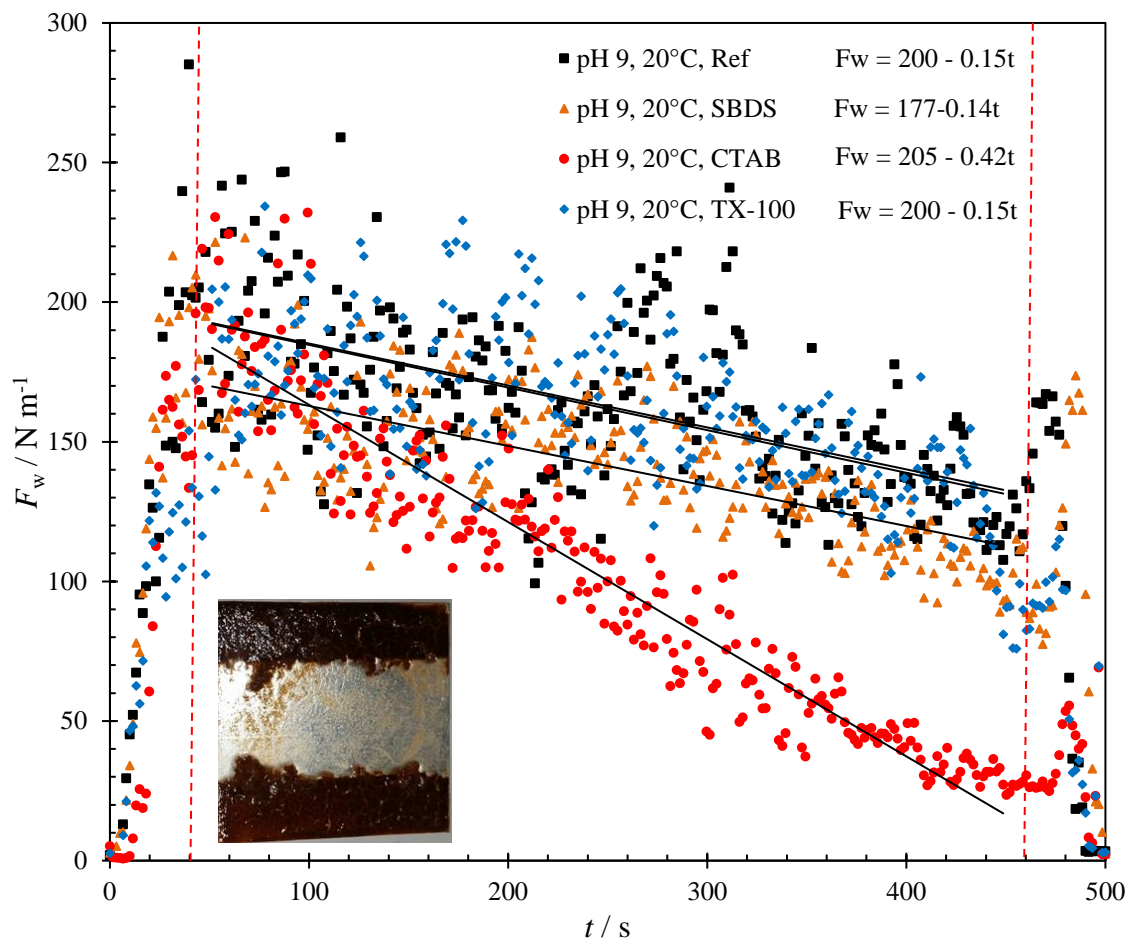
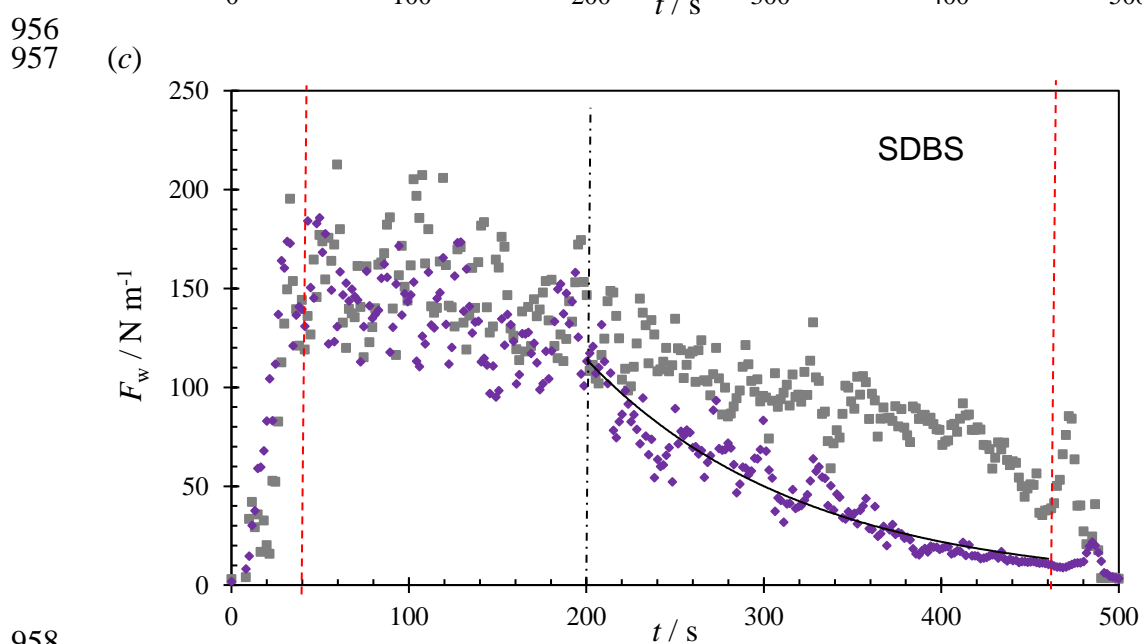
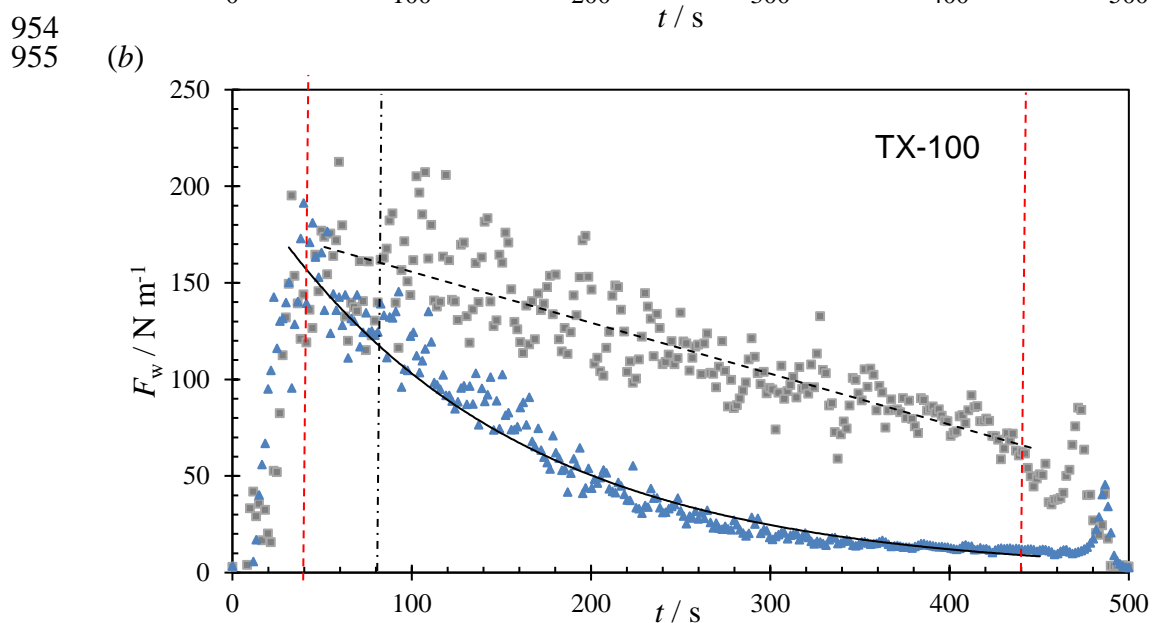
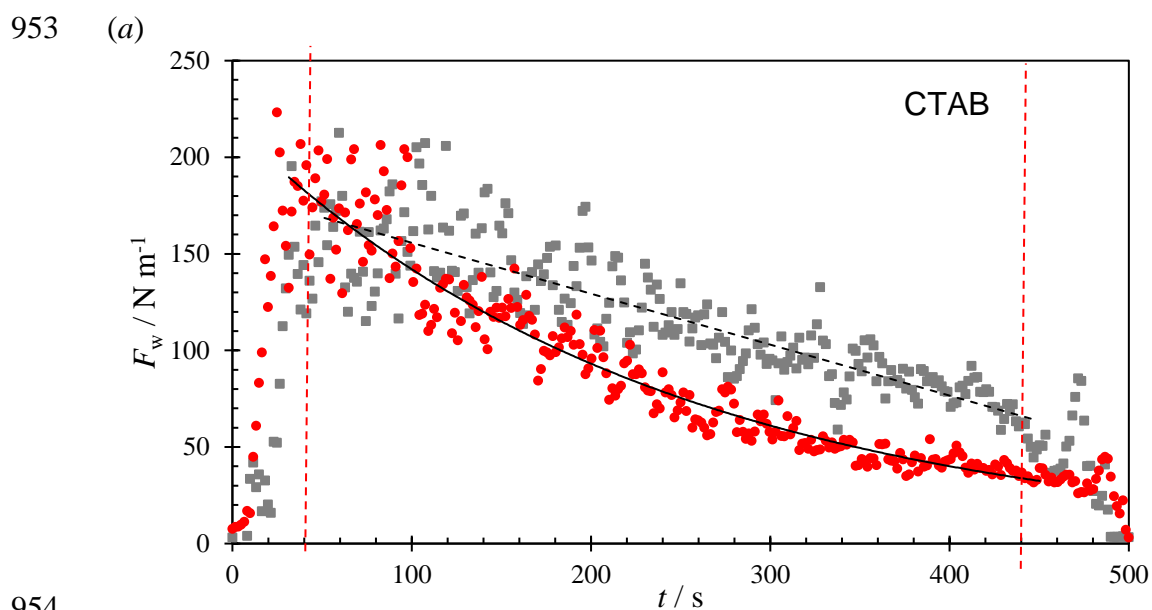


Figure 11: Effect of surfactant on removal force at 20 °C. Soil is contacted with pH 9 solution at  $t = 0$ . Lines show linear regression to data in the range  $50 < t < 350$  s. Vertical dashed lines mark initial and final regions subject to edge effects. Photograph shows cleared region after testing with CTAB solution.



958

959 Figure 12: Effect of 1 wt% surfactant on removal profiles at pH 9 and 50°C. (a) CTAB,  
960 (b) TX-100, (c) SDBS solution. Grey symbols show profile obtained without  
961 surfactant (Figure 10(a)). Vertical dashed lines mark initial and final regions  
962 subject to edge effects. Vertical dot-dash line marks B/C transition. Solid lines  
963 show fit of data in stage C to a simple exponential decay.

964

## Supplementary Figures

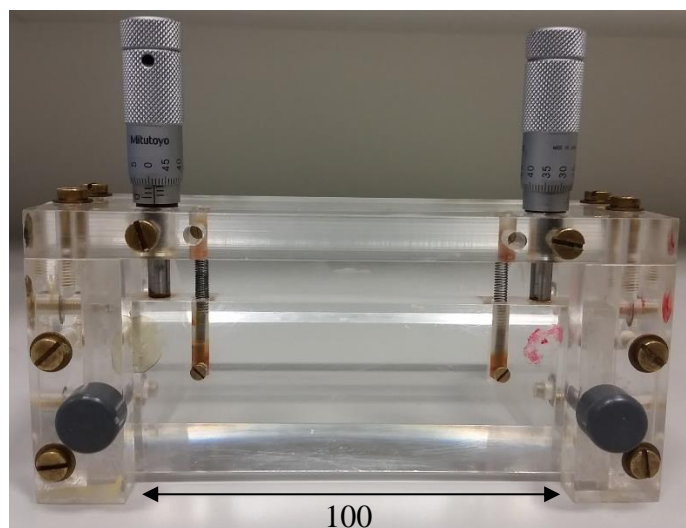
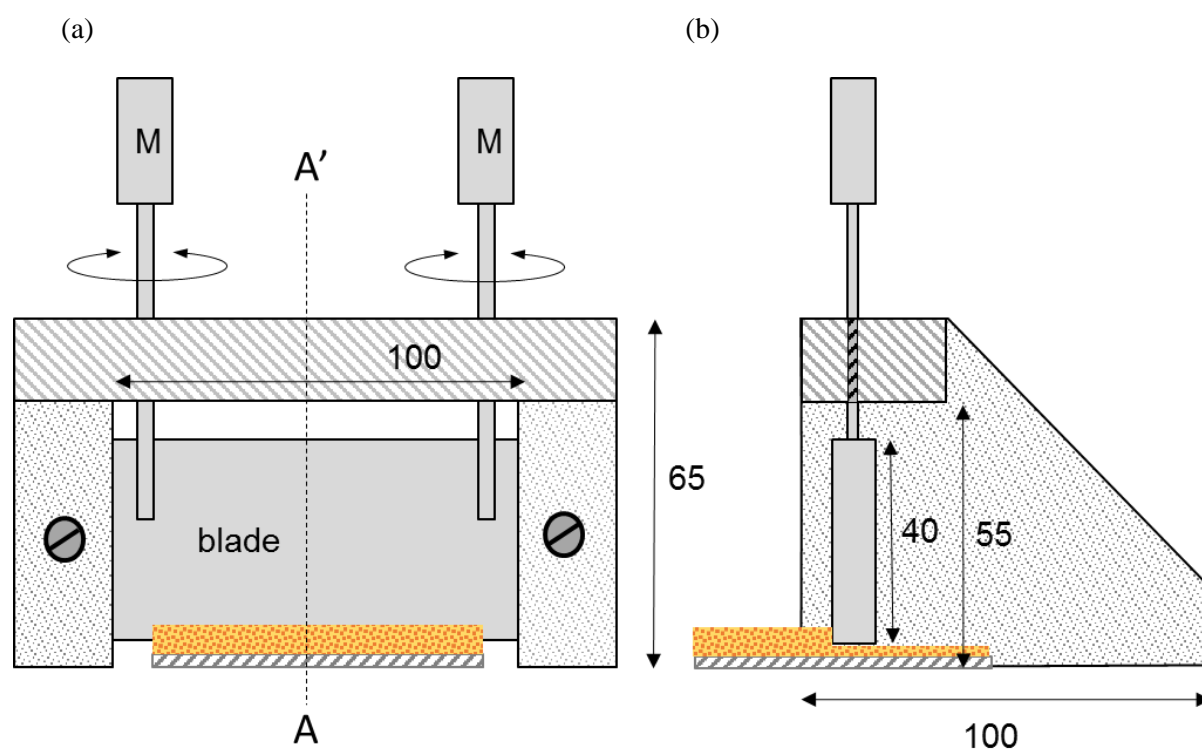
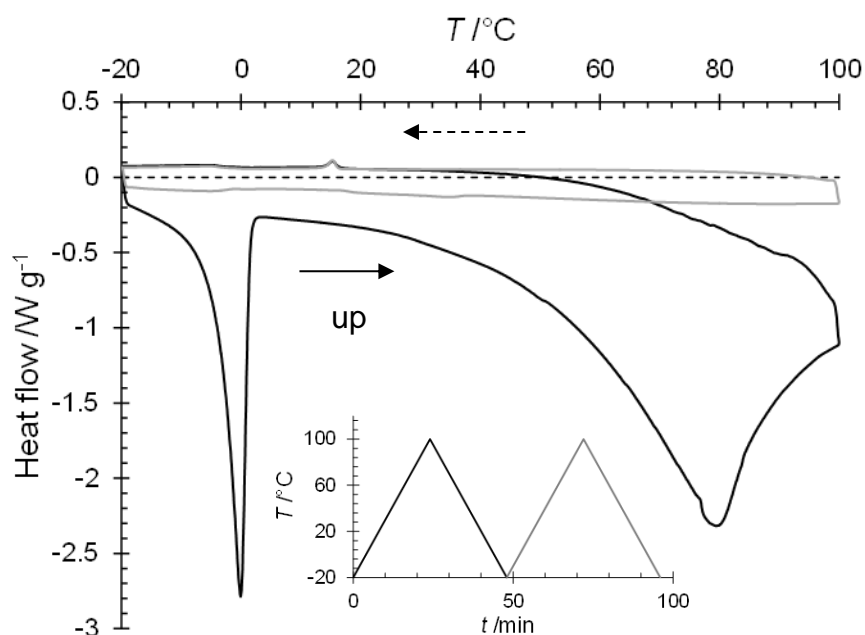
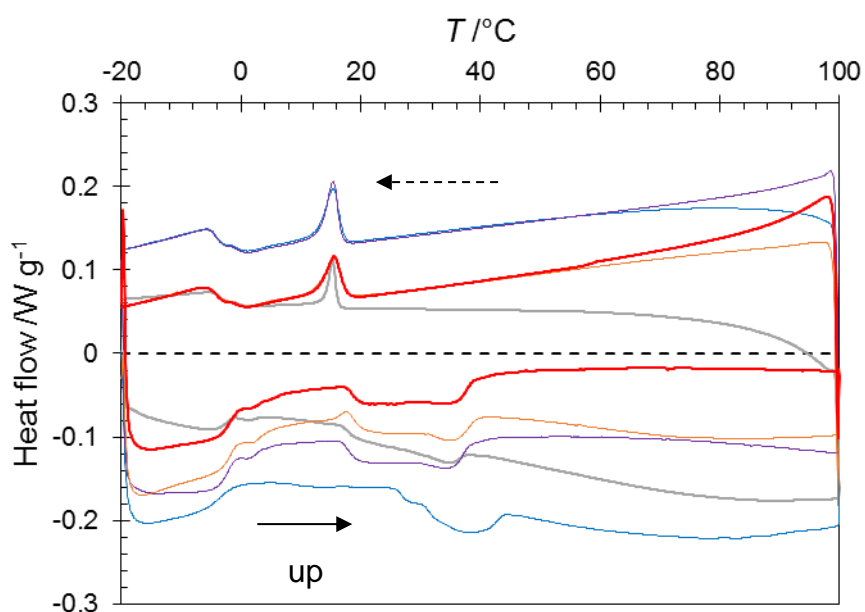


Figure S2: Schematic of sample spreading device. (a) front view; (b) section through plane AA'; (c) photograph. M indicates micrometers used to set the substrate-blade gap. Dimensions are in mm.

974 (a)

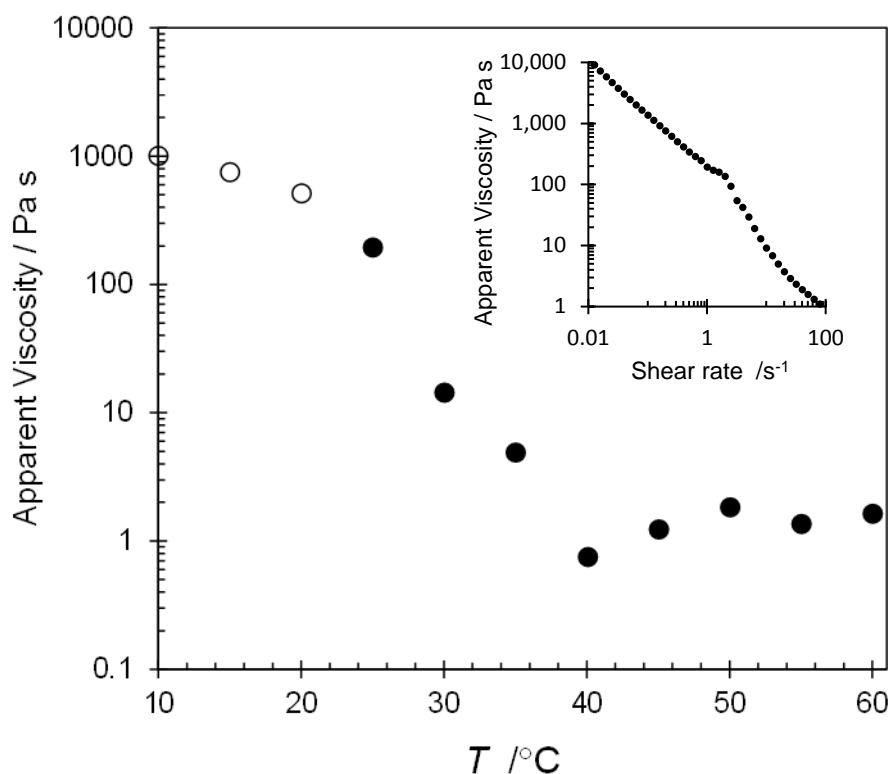


975  
976 (b)



977  
978

979 Figure S2: DSC thermograms of (a) fresh and (b) fresh, dried and burnt CMS.  
 980 Temperature ramped from -20 to 100 °C at 5 K min<sup>-1</sup> twice, as shown by inset  
 981 in (a). Fresh; black – scan 1, grey – scan 2. Dried; blue – scan 1, purple – scan  
 982 2. Burnt; orange – scan 1, red – scan 2.



984

985 Figure S3: Shear viscosity of fat component of CMS (40 % emulsion of fat in water).

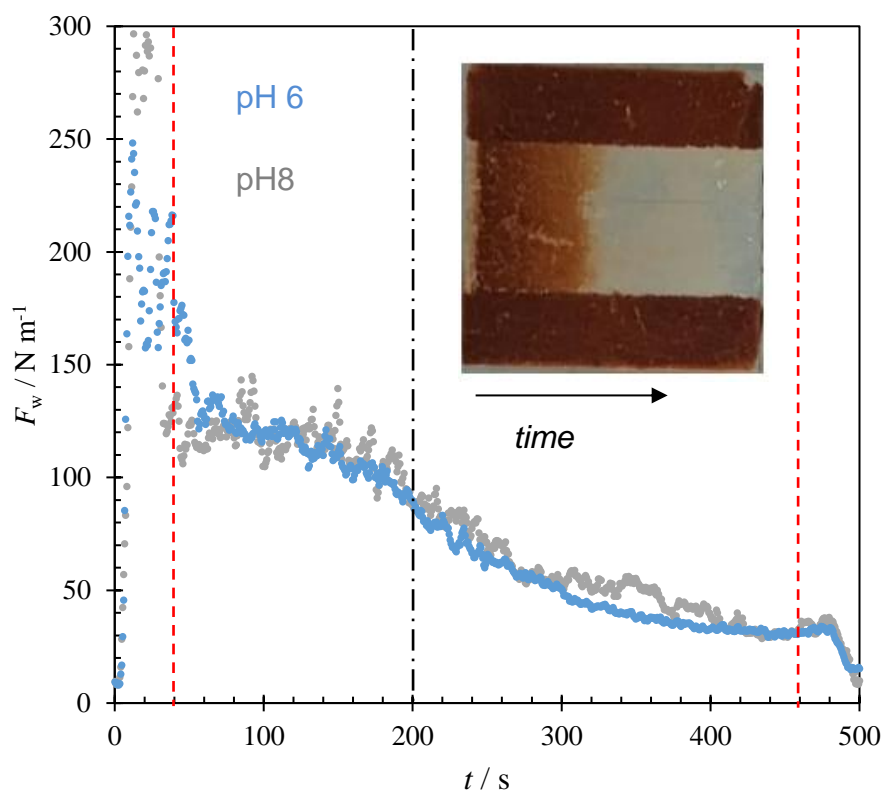
986 Apparent viscosity measured at apparent shear rate of 0.1 s⁻¹. Open symbols

987 indicate data with significant normal stress differences, indicating strongly non-

988 Newtonian behaviour. Inset shows the shear rate dependency at 22°C: below

989 0.1 s⁻¹ the gradient is close to -1, associated with yield stress behaviour.

990



991

992 Figure S4: Effect of pH on removal profiles at 50 °C. Blue pH 6  $D \sim 230$ , Grey pH 8  $D$   
 993  $\sim 220$ . Vertical dashed lines mark region A and D (edge effects). Dot-dashed  
 994 line marks B/C transition, observed at 200 s for both pH 6 and 8. Image shows  
 995 an example of the substrate after testing. Note:  $F_w$  in section B is lower than that  
 996 measured at pH 7 for a different CMS batch (Figure 8(b)).